CHAPTER 1

Background on Mechanics of Materials

CHAPTER 1.1

Background on Modeling

JEAN LEMAITRE
Université Paris 6 — LMT Cachan, 61 av. du président Wilson, F-94235 Cachan Cedex, France

Contents

1.1.1 INTRODUCTION

Modeling, as has already been said for mechanics, may be considered "a science, a technique, and an art."

It is science because it is the process by which observations can be put in a logical mathematical framework in order to reproduce or simulate related phenomena. In mechanics of materials constitutive equations relate loadings as stresses, temperature, etc. to effects as strains, damage, fracture, wear, etc.

Handbook of Materials Behavior Models

It is a technique because it uses tools such as mathematics, thermodynamics, computers, and experiments to build close form models and to obtain numerical values for the parameters that are used in structure calculations to predict the behavior of structures in the service or forming process, etc., safety and optimal design being the main motivations.

It is an art because the sensibility of the scientist plays an important role. Except for linear phenomena, there is not unique way to build a model from a set of observations and test results. Furthermore, the mathematical structure of the model may depend upon its use. This is interesting from the human point of view. But it is sometimes difficult to select the proper model for a given application. The simplest is often the more efficient event, even if it is not the most accurate.

1.1.2 OBSERVATIONS AND CHOICE OF VARIABLES

First of all, in mechanics of materials, a model does not exist for itself; it exists in connection with a purpose. If it is the macroscopic behavior of mechanical components of structures that is being considered, the basic tool is the mechanics of continuous media, which deals with the following:

1. Strain, a second-order tensor related to the displacement $\vec{u}$ of two points:

- Euler's tensor $\underline{\varepsilon}$ for small perturbations.

$$\varepsilon_{ij} = \frac{1}{2}\left(u_{i,j} + u_{j,i}\right) \tag{1}$$

  In practice, the hypothesis of "small" strain may be applied if it is below about 10%.
- Green-Lagrange tensor $\underline{\Delta}$ (among others) for large perturbations, if F is the tangent linear transformation which transforms under deformation a point M_0 of the initial configuration into M of the actual configuration.

$$\begin{aligned} d\vec{x}(M) &= \underline{F} d\vec{X}(M_0) \\ \underline{\Delta} &= \frac{1}{2}\left(\underline{F}^T \underline{F} - \underline{1}\right) \end{aligned} \tag{2}$$

  With $\underline{F}^T$ the transpose of $\underline{F}$.

2. Stress, a second-order tensor dual of the strain tensor; its contracted product by the strain rate tensor is the power involved in the mechanical process.

- Cauchy stress tensor σ for small perturbations, checking the equilibrium with the internal forces density $\vec{f}$ and the inertia forces $\rho\ddot{\vec{u}}$,

$$\sigma_{ij,j} + f_i = \rho\ddot{u}_i \quad \text{with } \ddot{u}_i = \frac{d^2u}{dt^2} \tag{3}$$

- Piola-Kirchoff tensor $\underline{S}$ (among others) for large perturbations.

$$\underline{S} = det(\underline{F})\underline{\sigma}\underline{F}^{-T} \tag{4}$$

3. Temperature T.

These three variables are functions of the time t.

1.1.2.1 Scale of Observation

From the mathematical point of view, strains and stresses are defined on a material point, but the real materials are not continuous. Physically, strain and stress represent averages on a fictitious volume element called the representative volume element (RVE) or mesoscale. To give a subjective order of magnitude of a characteristic length, it can be

≈ 0.1 mm for metallic materials;
≈ 1 mm for polymers;
≈ 10 mm for woods;
≈ 100 mm for concrete.

It is below these scales that observations must be done to detect the micromechanisms involved in modeling:

– slips in crystals for plasticity of metals;
– decohesions of sand particles by breaking of atomic bonds of cement for damage in concrete;
– rupture of microparticles in wear;
– etc.

These are observations at a microscale. It is more or less an "art" to decide at which microscale the main mechanism responsible for a mesoscopic phenomenon occurs. For example, theories of plasticity have been developed at a mesoscale by phenomenological considerations, at a microscale when dealing with irreversible slips, and now at an atomic scale when modeling the movements of dislocations.

At any rate, one's first priority is to observe phenomena and to select the representative mechanism which can be put into a mathematical framework

of homogenization to give variables at a mesoscale compatible with the mechanics of continuous media.

1.1.2.2 Internal Variables

When the purpose is structural calculations with sets of constitutive equations, it is logical to consider that each main mechanism should have its own variable. For example, the total strain $\underline{\varepsilon}$ is directly observable and defines the external state of the representative volume element (RVE), but for a better definition of the internal state of the RVE it is convenient to look at what happens during loading and unloading of the RVE to define an elastic strain $\underline{\varepsilon}^e$ and a plastic strain $\underline{\varepsilon}^p$ such as

$$\varepsilon_{ij} = \varepsilon^e_{ij} + \varepsilon^p_{ij} \tag{5}$$

The elastic strain represents the reversible movements of atoms, and the plastic strain corresponds to an average of irreversible slips.

All variables which define the internal state of the RVE are called internal variables. They should result from observations at a microscale and from a homogenization process:

- isotropic hardening in metals related to the density of dislocations;
- kinematic hardening related to the internal residual microstresses at the level of crystals;
- damage related to the density of defects;
- etc.

How many do we need? As many as the number of phenomena taken into consideration, but the smallest is the best.

Finally, the local state method postulates that the considered thermodynamic state is completely defined by the actual values of the corresponding state variables: observable and internal.

1.1.3 FORMULATION

The thermodynamics of irreversible processes is a general framework that is easy to use to formulate constitutive equations. It is a logical guide for incorporating observations and experimental results and a set of rules for avoiding incompatibilities.

The first principle is the energy balance: If e is the specific internal energy, ρ the density, ω the volume density of internal heat produced by external

sources, and $\vec{q}$ The heat flux:

$$\rho\dot{e} = \sigma_{ij}\dot{\varepsilon}_{ij} + \omega - q_{i,i} \tag{6}$$

The second principle states that the entropy production $\dot{s}$ must be larger or equal to the heat received divided by the temperature

$$\rho\dot{s} \geq \frac{\omega}{T} - \left(\frac{q_i}{T}\right)_{,i} \tag{7}$$

If $\psi = e - Ts$ is the Helmholtz specific free energy (this is the energy in the RVE which can eventually be recovered),

$$\sigma_{ij}\dot{\varepsilon}_{ij} - \rho(\dot{\psi} + s\dot{T}) - \frac{q_i T_{,i}}{T} \geq 0 \tag{8}$$

This is the Clausins-Duhem inequality, which corresponds to the positiveness of the dissipated energy and which has to be fulfilled by any model for all possible evolutions.

1.1.3.1 State Potential

The state potential allows for the derivation of the state laws and the definition of the associate variables or driving forces associated with the state variables V_K to define the energy involved in each phenomenon. Choosing the Helmholtz free energy ψ, it is a function of all state variables concave with respect to the temperature and convex with respect to all other V_K,

$$\psi = \psi(\underline{\varepsilon}, T, \varepsilon^e, \underline{\varepsilon}^p, \ldots V_K \ldots) \tag{9}$$

or in classical elastoplasticity

$$\psi = \psi(\underline{\varepsilon}^e, \underline{\varepsilon}^p, T, \ldots V_K \ldots) \tag{10}$$

The state laws derive from this potential to ensure that the second principle is always fulfilled.

$$\sigma_{ij}\dot{\varepsilon}^p_{ij} - \sum \rho \frac{\partial\psi}{\partial V_K}\dot{V}_K - \frac{q_i T_{,i}}{T} \geq 0 \tag{11}$$

They are the laws of thermoelasticity

$$\sigma_{ij} = \rho \frac{\partial\psi}{\partial\varepsilon^e_{ij}} \tag{12}$$

$$s = -\frac{\partial\psi}{\partial T} \tag{13}$$

The associated variables are defined by

$$\sigma_{ij} = \rho \frac{\partial \psi}{\partial \varepsilon^p_{ij}} \tag{14}$$

$$A_K = \rho \frac{\partial \psi}{\partial V_K} \tag{15}$$

Each variable A_K is the main cause of variation of the state variable V_K. In other words, the constitutive equations of the phenomenon represented by V_K will be primarily a function of its associated variable and eventually from others.

$$\dot{V}_K = g(\ldots A_K \ldots) \tag{16}$$

They also allow us to take as the state potential the Gibbs energy dual of the Helmholtz energy by the Legendre-Fenchel transform

$$\psi^* = \psi^*(\underline{\sigma}, s, \ldots A_K \ldots) \tag{17}$$

or any combination of state and associated variables by partial transform.

1.1.3.2 Dissipative Potential

To define the g function of the kinetic equations, a second potential is postulated. It is a function of the associate variables, and convex to ensure that the second principle is fulfilled. It can also be a function of the state variables but taken only as parameters.

$$\varphi = \varphi(\underline{\sigma}, \ldots A_K \ldots, \overrightarrow{\text{grad}}\, T; \underline{\varepsilon}^e, T, \ldots V_K \ldots) \tag{18}$$

The kinetic laws of evolution of the internal state variables derive from

$$\dot{\varepsilon}^p_{ij} = \frac{\partial \varphi}{\partial \sigma_{ij}} \tag{19}$$

$$\dot{V}_K = -\frac{\partial \varphi}{\partial A_K} \tag{20}$$

$$\frac{\vec{q}}{T} = -\frac{\partial \varphi}{\partial \overrightarrow{\text{grad}}\, T} \tag{21}$$

Unfortunately, for phenomena which do not depend explicitly upon the time, this function is not differentiable. The flux variables are defined by the subdifferential of φ. If F is the criterion function whose the convex $F = 0$ is the

indicatrice function of φ.

$$\begin{cases} \varphi = 0 & \text{if} \quad F<0 \rightarrow \dot{\underline{\varepsilon}}^p = 0 \\ \varphi = \infty & \text{if} \quad F = 0 \rightarrow \dot{\underline{\varepsilon}}^p \neq 0 \end{cases} \tag{22}$$

Then, some mathematics prove that

$$\begin{aligned} \dot{\varepsilon}_{ij}^p &= \frac{\partial F}{\partial \sigma_{ij}} \dot{\lambda} \\ \dot{V}_K &= -\frac{\partial F}{\partial A_K} \dot{\lambda} \end{aligned} \quad \text{if} \quad F = 0 \quad \text{and} \quad \dot{F} = 0 \tag{23}$$

$$\begin{aligned} \dot{\varepsilon}_{ij}^p &= 0 \\ \dot{V}_K &= 0 \end{aligned} \quad \text{if} \quad F<0 \quad \text{or} \quad \dot{F}<0 \tag{24}$$

This is the generalized normality rule of standard materials for which $\dot{\lambda}$ is the multiplier calculated by the consistancy condition $f = 0, \dot{f} = 0$.

1.1.4 IDENTIFICATION

The set of constitutive equations is fully defined if the two potentials ψ and ϕ take appropriate close forms: this is the qualitative identification. The numerical response of the constitutive equations to any input is obtained if the materials parameters take the appropriate values: this is the quantitative identification.

1.1.4.1 Qualitative Identification

Assume an interest in several phenomena for which q internal variables have been identified. Which functions should one choose for $\psi(\underline{\varepsilon}^e, \underline{\varepsilon}^p, T, V_1 \ldots V_q)$ and $\varphi(\underline{\sigma}, A_1 \ldots A_q, \overrightarrow{\text{grad}}\, T; \underline{\varepsilon}^e, T, V_1 \ldots V_q)$?

If a phenomenon is known as linear, the corresponding potentials are positive definite quadratic functions. For linear elasticity, for example,

$$\psi_e = \frac{1}{2\rho} E_{ijkl} \varepsilon_{ij}^e \varepsilon_{kl}^e \tag{25}$$

where ρ is the density and $\underline{\underline{E}}$ the Hooke tensor.

If two phenomena I and J are known to be coupled, the corresponding potentials should verify

- a state coupling: $\partial^2\psi/\partial V_I \partial V_J \neq 0$
- or an evolution coupling: $\partial^2\varphi/\partial V_I \partial V_J \neq 0$

If no coupling occurs $\partial^2\psi/\partial V_I \partial V_J = 0$ and $\partial^2\varphi/\partial V_I \partial V_J = 0$.

Following is an example of elasticity coupled to damage represented by the variable D:

$$\frac{\partial^2 \psi}{\partial D \partial \varepsilon_{ij}^e} \neq 0 \tag{26}$$

$$\psi_e = \frac{1}{2\rho} E_{ijkl} \varepsilon_{ij}^e \varepsilon_{kl}^e \cdot H_1(D) \quad \leftarrow \text{multiplication of functions} \tag{27}$$

$$\sigma_{ij} = \rho \frac{\partial \psi_e}{\partial \varepsilon_{ij}^e} = E_{ijkl} \varepsilon_{ij}^e \cdot H_1(D) \tag{28}$$

If such coupling would not have existed, we would have written

$$\psi_e = \frac{1}{2\rho} E_{ijkl} \varepsilon_{ij}^e \varepsilon_{kl}^e + H_2(D) \quad \leftarrow \text{addition of functions} \tag{29}$$

that is, $\partial^2 \psi / \partial D \partial \varepsilon_{ij}^e = 0$

$$\sigma_{ij} = \rho \frac{\partial \psi_e}{\partial \varepsilon_{ij}^e} = E_{ijkl} \varepsilon_{ij}^e \tag{30}$$

For nonlinear phenomena, often power functions are used, but for phenomena which asymptotically saturate, exponential functions are preferred. Often this choice is subjective. Nevertheless, micromechanics analysis may yield logical functions with regard to the micromechanisms introduced at microscale. It consists of the calculation of the energy involved in a RVE by a proper integration or an average of the elementary energies corresponding to the micromechanisms considered.

Qualitative experiments are used to point out the tendencies of evolution, but they do not concern the potentials in themselves because simple direct measurements of energy is not possible. Measurements concern the evolution of variables: strain as a function of stress, crack length as a function of time, etc. This means that the potentials are identified from an integration of what is observed. For example, an observation of the secondary creep plastic strain rate as a nonlinear function of the applied stress in creep tests given by the phenomenological Norton law $\dot{\varepsilon}_p = (\sigma/K)^N$ is introduced in the dissipative potential as

$$\varphi = \frac{K}{N+1} \left(\frac{\sigma_{eq}}{K} \right)^{N+1} \tag{31}$$

if some multiaxial experiments show that the von Mises criterion is fulfilled (σ_{eq} is the von Mises equivalent stress).

1.1.4.2 Quantitative Identification

This is the weakest point of the mechanics of materials. All the parameters introduced in constitutive equations (Young's modulus E and Poisson's ratio v in elasticity, Norton's parameters K and N in creep, etc.) differ for each material and are functions of the temperature. Since there are thousands of different materials used in engineering and since they change with the technological progress of elaboration processes, there is no way to built definite, precise databases. Another point is that when a structural calculation is performed during a design, the definitive choice of materials is not achieved, and, even if it is, nobody knows what the precise properties of the materials elaborated some years after will be. The only solution is to perform the structural calculations with the models identified with all known information and to update the calculations each time a new piece of information appears, even during the service of the structure. This, of course, necessitates close cooperation between the designers and the users.

1.1.4.2.1 Sensibility to Parameters

When a model is being used, all material parameters do not have the same importance for the results: a small variation of some of them may change the results by a large amount, whereas a large variation of others has a small influence. For example, a numerical sensibility analysis on the parameters σ_y, K, and M on the shape of the stress-strain curve, graph of the simple model of uniaxial plasticity

$$\sigma = \sigma_y + K\varepsilon_p^{1/M} \tag{32}$$

shows that the more sensible parameter is σ_y; by taking an approximate value of M ($M = 3, 4, 5$), it is always possible to adjust K in order to have a satisfactory agreement. But a good correlation with the set of available data does not prove that the model is able to give satisfactory results for cases far away from the tests used for the identification.

Before any quantitative identification of a model is made, it is advisable to perform a sensibility analysis in order to classify by increasing order of sensibility the parameters σ_y, K, and M and to proceed as follows:

1.1.4.2.2 Rough Estimation of Parameters

From all known data, make a first estimation of the parameters using all approximations in the model in order to have the same number of unknowns as the number of pieces of information. Eventually, take values of parameters corresponding to materials that are close in their chemical composition.

Continue with the same example of the preceding plasticity model for a mild steel for which σ_y is known as 300 MPa. If the ultimate stress σ_u is known as 400 MPa for a plastic strain to rupture $\varepsilon_{pu} \approx 0.20$, then taking $M = 1$ allows one to find $K \approx 500$ MPa.

These approximate values of the parameters may be taken as a starting solution of an optimization process.

1.1.4.2.3 Optimization Procedure

If now more experimental results are available, an optimization procedure may be performed to minimize the difference between the test data and the prediction of those tests by the full numerical resolution of the model. The least-square method is advantageously used.

Unfortunately, in the range of nonlinear models, the minimization of the error function may have several solutions due to local minima or flat variations for which the gradient methods converge extremely slowly. This is why the starting solution should be as close as possible to the optimized solution and why one should give different weight factors to the parameters in order "to help" the numerical procedure: small weight factors to less sensible parameters.

1.1.4.2.4 Validation

The process is not finished until the model has been applied and compared to special tests which have not been used for the identification. Of course, the model should be applied to the identification cases, but this is only for checking the identification procedure.

These validation tests must be as close as possible to the case considered for applications, and as far as possible from the identification tests — close or far in the sense of variables. For example:

- biaxial tests if the tests of identification were uniaxial;
- nonisothermal tests if the tests of identification were conducted at constant temperature;
- tests with gradient of stress or of other variables;
- different time scales;
- etc.

The comparison between validation tests and prediction gives concrete ideas about the applicability of the models from the point of view of accuracy and robustness.

1.1.5 VALIDITY DOMAIN

Sometimes people say that "a good model should only be used to interpolate between good tests." I do not agree with this pessimistic view because to interpolate between tests results a "good polynome" is sufficient. A model is something more. First, it includes ideas on the physical mechanisms involved; second, it is a logical formulation based on general concepts; and third, only after that, it is numbers.

The domain of validity of a model is the closed domain in the space of variables inside which any resolution of the model gives an acceptable accuracy. For the preceding model of plasticity, this is $0 < \sigma < 400\,\text{MPa}$, $0 < \varepsilon_p < 0.2$ for a relative accuracy of about $\delta\varepsilon_p/\varepsilon_p \approx 10\%$ on plastic strain for a given stress.

The bounds are difficult to determine; they are those investigated by the identification tests program, plus "motivated" extrapolations based on well-established concepts. Time extrapolation is the most crucial because the identification procedure deals within a time range of hours, days, or months, whereas the applications of models deal within a time range of years or decades. In such long periods of time phenomena of aging and changing properties can occur which may be not included in the models. Aging and change of properties by "in-service incidents" are certainly still open problems.

1.1.6 CHOICE OF MODELS

The best model for a given application must be selected with much care and critical analysis. First of all, investigate all the phenomena which may occur and which have to be checked in the application: for example, monotonic or cyclic plasticity.

Then determine the corresponding variables which should exist in the model: for example, cyclic plasticity needs a kinematic hardening variable.

Check the domain of validity of the possible models in comparison to what is expected in the application and select the simplest that has a good ratio of quality to price, the quality being the accuracy and the price the number of materials parameters to identify.

The choice of the model depends also on the available data to identify the material parameters for the material concerned. Fortunately, often the structural calculations are performed to compare different solutions in order to optimize a design. In that case, good qualitative results are easily obtained with rough estimations of the parameters.

1.1.7 NUMERICAL IMPLEMENTATION

The last activity in modeling is the numerical use of the models. Most of them, in mechanics of materials, are nonlinear, incremental procedures and are used together with iterations. For example, in plasticity:

- In a first step the incremental strain field is calculated by means of the kinetic equations from momentum equations.
- The second step concerns the integration of the constitutive equations to obtain the increments of the state variables and their new values.
- The third step consists in checking the momentum balance equation for the actual stresses; if violated the iteration process goes to step 1 until a given accuracy is obtained.

The Newton-Raphson method is often used. Implicit schemes in quasi-static conditions or explicit schemes in dynamic conditions are used until the end of the loading history or if a divergence appears as a loss of ellipticity or a strain localization characteristic of softening behavior.

BIBLIOGRAPHY

Ashby, M., and Jones, D. (1987). *Engineering Materials*, vols. 1 and 2, Pergamon.

François, D., Pineau, A., and Zaoui, A. (1998). *Mechanical Behavior of Materials*, vols. 1 and 2, Kluwer Academic Publishers.

Lemaitre, J., and Chaboche, J. L. (1995). *Mechanics of Solid Materials*, Cambridge: Cambridge University Press.

CHAPTER 1.2

Materials and Process Selection Methods

YVES BRECHET
38402 St Martin d'Heres Cedex, France

Contents

1.2.1 INTRODUCTION

Designing efficiently for structural applications requires both a proper dimensioning of the structure (involving as a basic tool finite element calculations) and an appropriate choice of the materials and the process used to give them the most suitable shape. The variety of materials available to the engineer (about 80,000), as well as the complex set of requirements which define the most appropriate material, lead to a multicriteria optimization problem which is in no way a trivial one. In recent years, systematic methods for materials and process selection have been developed [1–4] and

Handbook of Materials Behavior Models

implemented into selection softwares [5–7] which ideally aim at selecting the best materials early enough in the design procedure so that the best design can be adequately chosen. This selection guide is most crucial at the early stages of design: there would be no hope of efficiently implementing a polymer matrix composite solution on a design initially developed for a metallic solution. Selecting the most appropriate materials is a task which should be done at the very beginning of the design procedure and all along the various steps, from conceptual design to detail design through embodiment design. The coupling with other design tools should at the very least provide finite element codes with constitutive behavior for the materials which appear the most promising. A more ambitious program, yet to be implemented, is to interface these elements with expert systems which would guide the designer toward shapes, processes more suited to a given class of materials, and which ultimately would help to redesign the component in an iterative manner according to the materials selection.

These methods require databases of materials and tools to objectively compare materials for a given set of requirements. The amount of modeling needed in these methods is still quite elementary. In the present paper, we will focus on the tools used to compare materials rather than on their implementation as computer software. The modeling involved in the performance index method (Section 1.2.2) is standard strength of materials. The search for an optimal solution sometimes requires more refined optimization techniques (Section 1.2.3). We will outline in Section 1.2.4 the possible use of micromechanics and optimization methods in the development of materials with the aim of meeting a giving set of requirements. In Section 1.2.5 we will illustrate the need to structure and store the expertise in process selection, and will outline the need for modeling in this area.

1.2.2 DATABASES: THE NEED FOR A HIERARCHICAL APPROACH

Material selection methods are facing a dilemma: the structure of the databases and the selection tools have to be as general as possible to be easily adaptable to a variety of situation. But this general structure is bound to fail when the selection problem is very specific (such as, for instance, selecting cast alloys). The methodology for materials selection presented in this paper is a compromise in this dilemma. We will present first the generic approach, and then some specific applications. The idea is always to go from the

most generic approach to the most specific one. In order to do so, the materials databases have to be organized in a hierarchical manner so that the selection at a given level orients the designer toward a more specific tool.

Depending on the stages of design at which one considers the question of materials selection, the level of information required will be different [1]. In the very early stages, all possible materials should be considered, and therefore a database involving all the materials classes is needed. Accordingly, at this level of generality, the properties will be stored as ranges with relatively low precision. When the design procedure proceeds, more and more detailed information is needed on a number of materials classes diminishing. Properties more specific to, say, polymers (such as the water intake or the flammability) might be referred to in the set of requirements. In the last stages of design, a very limited number of materials, and finally one material and a provider, have to be selected: at this lever, very precise properties suitable for dimensioning the structure are needed. This progressive increase in specialization motivates a hierarchical approach to databases used in materials selection tools: instead of storing all the possible properties for a huge number of materials, which is bound to lead to a database loaded with missing information, the choice has been to develop a series of databases incorporating each a few hundreds of materials. The generic database comprises metals, polymers, ceramics, composites, and natural materials. Specialized databases have been developed for steels, light alloys, polymers, composites, and woods. More specialized databases coupling the materials and the processes (such as cast alloys, or polymer matrix composites) can then be developed, but their format is different from the previous databases.

The set of requirements for structural applications is very versatile. Of course, mechanical properties are important (such as elastic moduli, yield stresses, fracture stresses, or toughness). These properties can be stored as numerical values. But very often, information such as the possibility of getting the materials as plates or tubes, the possibility of painting or joining it with other materials, or its resistance to the environment chemically aggressive are as important. All the databases currently developed contain numerical information, qualitative estimates, and boolean evaluations. More recent tools [6] also allow one to store not only numbers, but also curves (such as creep curves for polymers, at a given temperature under a given strength). When a continuum set of data has to be stored, such as creep curves or corrosion rates, being able to rely on a model with a limited number of parameters (such as Norton's law for creep) considerably increases the efficiency of the storing procedure. For a database to be usable for selection purposes, it should be complete (sometimes needing some estimation

procedure), it should not overemphasize one material with respect to the others, and it should contain data which are meaningful for all the materials in the database.

The databases used in materials selection are of two types: either they list the materials which are possible candidates, or they store the elements from which the possible candidates are made. The first case is rather simple; provided a correct evaluation function is defined, the ranking of the candidates can be done by simple screening of the database. The second case, for instance, when the database lists the resins and the fibers involved in making a composite material, requires both micromechanical tools to evaluate the properties of the materials from the ones of its components, and also more subtle numerical methods that are able to deal with a much larger (virtually infinite) set of possible candidates. Steepest gradient methods, simulated annealing, and genetic algorithms are possible solutions for these complex optimization problems.

In principle, one should try to select materials and processes simultaneously, since it is very often in terms of competition between various couples (materials/processes) that the selection problem finally appears: should one make an aiplane wing joining components obtained from medium-thickness plates of aluminum alloys, or should one machine inside a thick plate of a less quench sensitive alloy the wing together with the stiffeners? The coupling between processes and materials properties is still very poorly taken into account in the current selection procedures. Processes are also selected from databases of attributes for the different processes (such as the size of the components, the dimensional accuracy, or the materials accessible to a given process). The databases for process attributes have the same structure as the ones for materials, and the same hierarchical organization, and information can be numeric, qualitative, or boolean.

Beside the variety of properties (for materials) and attributes (for processes) involved in a selection procedure, depending on the stage of selection, one is either confronted with a very open end set of requirements, or with always the same set of questions. In the first situation, one needs a very versatile tool, but because of combinatoric explosion, one cannot afford to deal with questions involving interactions that are too complex between various aspects, (such as "this shape, for this alloy, assuming this minimal dimension, is prone during casting to exhibit hot tearing"). On the other hand, when the selection becomes very focused (such as selection of joining methods), the set of requirements to be fulfilled has basically always the same format: it can be stored as a "predefined questionnaire" which allows more refined questions to be asked since they are in a limited number.

1.2.3 COMPARING MATERIALS: THE PERFORMANCE INDEX METHOD

The databases are the hard core of the selection procedure: up to a certain point they can be cast in a standard format, which has been used in CMS, CPS, and CES software. When selection reaches a high degree of specialization, more specific formats have to be implemented, and a questionnaire approach rather than an "open-end selection" might be more efficient. But a database would be of little use without an evaluation tool able to compare the different materials. Simple modeling allows one to build such a tool, but the price to be paid is that dimensioning of the structure using this method is very crude. One has to keep in mind that the aim is to identify the materials for which accurate structural mechanics calculations will have to be performed later on.

Each set of requirements has to be structured in a systematic manner: What are the constraints? What are the free and the imposed variables? What is the objective? For instance, one might look for a tie for which the length L is prescribed and the section S is free (free and imposed dimensions), which shouldn't yield under a prescribed load P (constraints), and which should be of minimum weight (objective). The stress which should not exceed the yield stress is

$$\frac{P}{S} \leq \sigma_y \tag{1}$$

The mass of the component to be minimized is

$$M = \rho.L.S \tag{2}$$

The constraint not to yield imposes a minimum value for the section S. The mass of the component is accordingly at least equal to

$$M_{\min} = \left(\frac{\rho}{\sigma_y}\right) \cdot (L.P) \tag{3}$$

Therefore, the material which will minimize the mass of the component will be the one which maximizes the "performance index" I:

$$I = \frac{\sigma_y}{\rho} \tag{4}$$

This very simple derivation illustrates the method for obtaining performance indices: write the constraint and the objectives, eliminate the free variable, and identify the combination of materials properties which measures the efficiency of materials for a couple (constraints/objectives). These performance indices have now been derived for many situations corresponding to simple geometry (bars, plates, shells, beams) loading in simple modes (tension, torsion, bending), for simple constraints (do not yield, prescribed

stiffness, do not buckle...), and for various objectives (minimum weight, minimum volume, minimum cost). They have been extended to thermal applications. The way to derive a performance index for a real situation is to:

- simplify the geometry and the loading;
- identify the free variables;
- make explicit the constraint using simple mechanics;
- write down the objective; and
- eliminate the free variables between the constraint and the objectives.

TABLE 1.2.1 Classical performance indices for mechanical design for strength or stiffness at minimum weight.

Objective	Shape	Loading	Constraint	Performance index
Stiffness design with a minimal mass				
Minimize the mass	Tie	Tension	Stiffness and length prescribed, section free	E/ρ
Minimize the mass	Beam	Bending	Stiffness, shape and length fixed, section free	$E^{1/2}/\rho$
Minimize the mass	Beam	Bending	Stiffness, width and length fixed, height free	$E^{1/3}/\rho$
Minimize the mass	Plate	Bending	Stiffness length width fixed, thickness free	$E^{1/3}/\rho$
Minimize the mass	Plate	Com-pression	Buckling load fixed, length width fixed, thickness free	$E^{1/3}/\rho$
Minimize the mass	Cylinder	Internal pressure	Imposed maximum elastic strain, thickness of the shell free	E/ρ
Strength design with a minimal mass				
Minimize the mass	Tie	Traction	Strength, length fixed, section free	σ_e/ρ
Minimize the mass	Beam	Bending	Strength, length fixed, section free	$\sigma_e^{2/3}/\rho$
Minimize the mass	Plate	Bending	Strength, length and width fixed, thickness free	$\sigma_e^{1/2}/\rho$
Minimize the mass	Cylinder	Internal pressure	Imposed pressure, the materials shall not yield, thickness of the shell free	σ_e/ρ

Table 1.2.1 gives some standard performance indices currently used in mechanical design. Many others have been derived, both for mechanical and thermo-mechanical loading [1, 4].

A simple way to use the performance index is with the so-called selection maps shown in Figure 1.2.1: on a logarithmic scale the lines corresponding to equal performances are straight lines whose slopes depend on the exponents entering the performance index. Figure 1.2.1 shows one of these maps used for stiff components at minimum mass. Materials for stiff ties should maximize E/ρ, materials for stiff beams should maximize $E^{1/2}/\rho$, and materials for stiff plates should maximize $E^{1/3}/\rho$.

These performance indices have a drawback, however: they are concerned with time-independent design, the component is made so that it

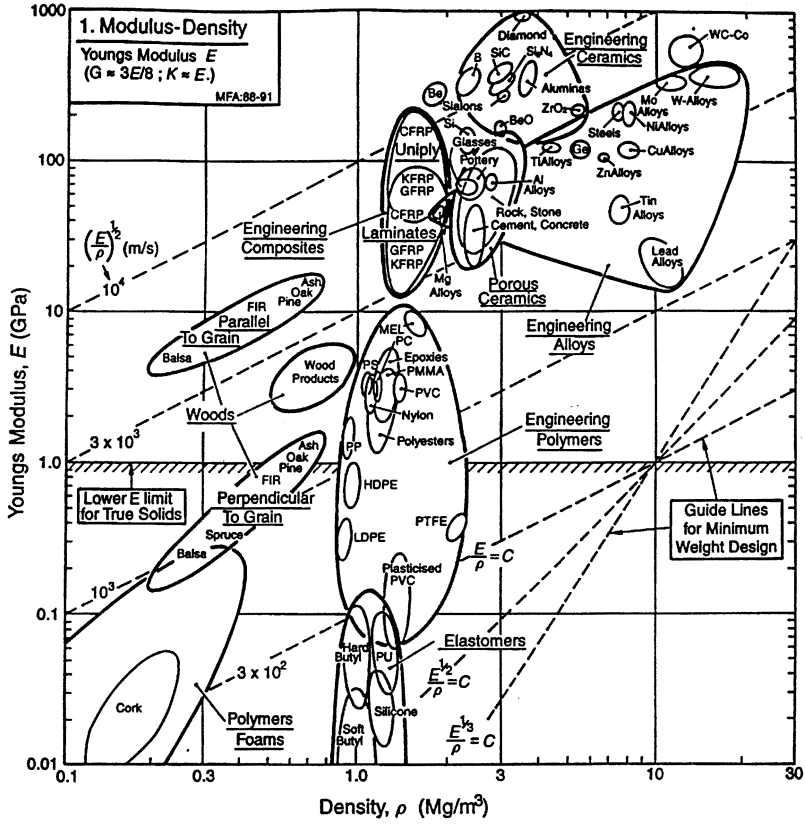

FIGURE 1.2.1 Selection map for stiff light design [1].

should fulfill its function when it starts being used, and it is assumed it will be so for the rest of its life. Of course, this is rarely the case, and one often has to design for a finite lifetime. As a consequence, for instance, in designing for creep resistance or corrosion resistance, a new set of performance indices involving rate equations (for creep or corrosion) has been developed [8, 9]. The performance indices then depend not only on the materials properties, but also on operating conditions such as the load, or the dimensions, or the expected lifetime. For instance, large-scale boilers are generally made out of steel, whereas small-scale boilers are often made in copper. In principle, finite lifetime design is possible within the framework of performance indices, but the data available to effectively apply the method are much more difficult to gather systematically.

1.2.4 THE DESIGN PROCEDURE: SCREENING, RANKING, AND FURTHER INFORMATION, THE PROBLEM OF MULTIPLE CRITERIA OPTIMIZATION

The previous method allows one to compare very different materials for a given set of requirements formulated as a couple (constraint/objective). However, in realistic situations, a set of requirements comprises many of these "elementary requirements." Moreover, only part of the requirements can indeed be formated that way. A typical selection procedure will proceed in three steps:

1. At the screening stage, materials will be eliminated according to their properties: only those that could possibly do the job will remain. For instance, for a component in a turbine engine, the maximum operating temperature should be around 800C: many materials won't be able to fulfill this basic requirement, and can be eliminated even without looking for their other properties.
2. At the ranking stage, a systematic use of performance indices is made: the problem is then, among admissible materials, to find the ones which will do the job most efficiently, that is, at the lowest cost, with the lowest mass, or the smallest volume. The ranking will be made according to a "value function" which encompasses the various aspects of the set of requirements. The problem of defining such a value function for multiple criteria optimization will be dealt with in the next paragraph.

3. For the remaining candidates that are able to fulfill the set of requirements efficiently, further information is often needed concerning corrosion rates, wear rates, or possible surface treatments. These pieces of information are scattered in the literature, and efficient word-searching methods are required to help with this step. At the same step, the local conditions, or the availability of the different possible materials, will also be a concern.

The three steps in the selection procedure are also a way to structure process selection. The screening stage will rely on attributes such as the size of the component and the materials from which it is made. The ranking step will need a rough comparative economic evaluation of the various processes, involving the batch size and the production rate. The last step will depend on the availability of the tooling and the will to invest.

It appears from these various aspects of the selection procedure that a key issue is to build a "value function" that is able to provide one with a fair comparison of the different possible solutions. The performance index method is the first step in building this value function. The second step is to deal with the multicriteria nature of the selection process. This multicriteria aspect can be conveniently classified in two categories: it might be a multiconstraint problem, or a multiobjective problem (in any real situations, it is both!). In a multiconstraint problem (such as designing a component which should neither yield nor fail in fatigue), the problem is to identify the limiting constraint. In order to do so, further knowledge on the load and the dimensions is needed. A systematic method called "coupled equations" [10] allows one to deal with this problem. In a multiobjective problem (such as designing a component at minimum weight and minimum cost), one needs to identify an "exchange coefficient" [10] between the two objectives, for instance, how much the user is ready to pay for saving weight. These exchange coefficients can be either obtained from a value analysis of the product or from the analysis of existing solutions [4]. They allow one to compute a value function, which is the tool needed to rank the possible solutions. Both the value analysis and the coupled equation method provide one with an objective treatment of the multiple criteria optimization. However, they require extra information compared to the simple performance index method. When this information is not available, one needs to make use of methods involving judgments. The most popular one is the "weight coefficients method," which attributes to each criteria a percentage of importance. The materials are then compared to an existing solution. It must be stressed that the value function so constructed depends on the choice of both the weighting factors and the reference material. Weighting factors are difficult to evaluate; moreover, multiple criteria often lead to no solution at all

due to an excessive severity. Multiple optimization also implies the idea of compromise between the various requirements. For this reason, algorithms involving fuzzy logic methods [3] have been developed to deal with the intrinsic fuzziness of the requirements (two values will be given, one above which the satisfaction is complete, one under which the material will be rejected). Proposed situations at the margin of full satisfaction will be proposed for evaluation, and the value function will be constructed so that it will give, for the same questions, the same evaluation as the user. This technique bypasses the difficulty in giving a priori value coefficients, since they are then estimated from the evaluation-proposed solutions. However, these methods still involve judgments (though in a controlled manner), and, when possible, the objective methods should be preferred.

Once the value function is available, the selection problem becomes an optimization one. When the database is finite, the optimization can be performed by a simple screening of all the available solutions. The method has been extended to the optimal design of multimaterials components such as sandwich structures [11, 12]. The aim is then to simultaneously select the skin, the core, and the geometry for a set of requirements involving stiffness and strength, constraints on the thickness, objectives on the weight, or the cost. For single criteria selection, an analytical method was derived [13]. For multiple criteria, such a method is no longer available, and the selection requires one to compute the properties of a sandwich from the properties of its components and its geometry, and to compare all the possible choices. In order to find the optimal solution, a genetic algorithm was used. The principle is to generate a population of sandwiches whose "genes" are the materials and the geometry. New sandwiches are generated, either by mutation or by crossover between existing individuals, and the population is kept constant in size by keeping the individuals alive with a greater probability when their efficiency (measured by the value function) is greater. In such a way, the algorithm converges very rapidly to a very good solution.

1.2.5 MATERIALS SELECTION AND MATERIALS DEVELOPMENT: THE ROLE OF MODELING

In the previous sections, we were interested in selecting materials and processes to fulfil a set of requirements. The only modeling needed at this stage is a simplified estimation of the mechanical behavior of the component, together with a clear identification of the constraints and the objectives. The value function allowing one to estimate the efficiency

of the different solutions is itself a simple linear combination of the performance indices corresponding to the dominant constraints identified by a predimensioning.

However, the same method has been applied to identify suitable materials whose development would fulfill the requirements. Composite materials are especially suitable for this exercise because their value relies partly on the possibility of tayloring them for application [14, 15]. In order to design a composite material, one has to identify the best choice for the matrix, for the reinforcement, for the architecture of the reinforcement and its volume fraction, and for the process to realize the component (which might be limited by the shape to be realized). One needs relations, either empirical or based on micromechanics models, between the properties of the components of the composite and the properties of the material itself. Usually, the process itself influences the properties obtained, which are lower than the properties of the ideal composite that micromechanics models would provide. One could think of introducing this feature in the modeling through interface properties, but it is generally more convenient to store the information as "knock-down factors" on properties associated with a triplet matrix/reinforcement/process. Another application of materials selection methods using mechanical modeling is the optimal design of glass compositions for a given set of requirements: since the properties are, within a certain range, linearly related to the composition, optimization techniques such as a simplex algorithm are well adapted to this problem. When a continuous variable, such as the characteristics of a heat treatment for an alloy, is available and is provided, either through metallurgical modeling or through empirical correlation, the properties can be given as a function of this variable, and materials selection methods are efficient to design the best treatment to be applied to fit a set of requirements. However, the explicit models available for relations between processes and properties are relatively few. Recent developments using Neural net-works to identify hidden correlation in databases of materials can also be applied and coupled to selection methods in order to design the best transformation processes.

Another recent development in selection methods aims at reverting the problem, that is, finding potential applications for new materials [4, 16, 17]. Several strategies have been identified: for instance, one can explore a database of applications (defined by a set of requirements and existing solutions) and find the applications for which the new material is better than the existing solutions. Another technique is to identify the performance indices for which the new material seems better than usual materials, and from there, to find out the applications for which these performance indices are relevant criteria.

1.2.6 PROCESS SELECTION: STRUCTURING THE EXPERTISE

In addition to selection by attributes of the process, which is efficient in the first stages of selection, when one is confronted with a more specific problem, such as selection of a definite cast aluminium alloy or a definite extruded wrought alloy, or selection of a secondary process such as joining or surface treatments, one is faced with the need to store expertise. For instance, for selection of cast aluminium [3, 18] alloys, the key issue is not to define the performance index; the key issue is to select the alloy which will be possible to cast without defects. Mold filling and hot tearing are the central concerns in this problem. The ability to fill a mold or to cast a component without cracks depends on the alloy, on the geometry of the mold, and on the type of casting. Ideally, one would wish to have models to deal with this question. In real life, hot tearing criteria are not quantitatively reliable, mold-filling criteria are totally empirical, and moreover, the properties of the cast alloy are dependent on the solidification conditions, that is, on the thickness of the component. These dependences are part of what is known as expertise. The simplest way to store this expertise is build the set of requirements according to a predefined questionnaire corresponding to the expert behavior. The second option is to mimic the general tendency identified by the expert by a simple mathematical function (for instance, capturing the tendency to increased hot tearing with thinner parts of the component) and to tune the coefficients of these functions by comparing the results of selection by a software with the results known from the case studies available to the expert. Along these lines, selection methods for cast alloys [18], extruded alloys [19], joining methods [20, 21], and surface treatments [4, 22] have been developed to capture various expertises. Clearly, modeling is still needed to rationalize the empirical rules commonly used (such as the shapes which can be extruded or cast), or to evaluate the cost of a process (for instance, for joining by laser, or for a surface treatment one needs to find the best operating temperature, power, speed, etc.).

1.2.7 CONCLUSIONS

The selection methods briefly presented in this chapter are recent developments. The use of modeling in these approaches is still in its infancy. In the last ten years, general methods and software have been developed to select materials, to select processes, and to deal with multidesign element conception and with multicriteria set of requirements.

TABLE 1.2.2 Selection softwares developed following the guidelines of the present paper.

Name of the software	Objectives of the software	Comments/status
CMS	Materials selection, graphical selection using maps; many databases, generic or specialized	Commercially available
CPS	Process selection, graphical method	Commercially available
CES	Materials and process selection, databases for materials, for processes and links between databases	Commercially available; constructor facility for development of dedicated databases
Fuzzymat	Materials selection, multicriteria and fuzzy logic-based selection algorithm	Commercially available; development of specialized databases
CAMD	Materials and process selection for multidesign element conceptions; expert system to guide and analyze the elaboration of requirements	
Fuzzycast	Selection of cast aluminium alloys; databases: alloys/processes/geometry	Property of Pechiney; expertise on casting processes, design rules
Fuzzy-composites	Design of polymer-based composites; databases: resin, reinforcements, processes, and compatibilities	
Sandwich selector	Optimization of sandwich structures; genetic algorithm coupled with fuzzy logic	
Fuzzyglass	Optimization of glass compositions; simplex coupled with fuzzy logic	Property of SaintGobain
Astek	Selection of joining methods; databases: processes and shapes	Property of CETIM
STS	Selection of surface treatments; database: processes/materials/objectives	
VCE	Evaluation of exchange coefficients from existing solutions	
MAPS	Investigation of possible applications for a new material	

Table 1.2.2 gives a list of selection tools developed along the philosophy described in this chapter. These generic methods have been specialized to various classes of materials and processes. In special situations, a coupling with modeling made possible the use of the present methods to develop new materials or new structures (composites, sandwich structures). For specific processes (casting, joining, extrusions, surface treatments), the selection procedure developed was closer to an expert system, following a predefined questionnaire. Various methods of finding applications for a new material have been put forward. Up to now, the choice has been to rely on empirical knowledge when available, and to keep the selection procedure as transparent and as objective as possible. The main reason for this paper to be included in a book on models in mechanics is to express the need now to couple more closely modeling to design so that one may go beyond empirical correlation and optimize both the choice of materials and their future development.

REFERENCES

1. Ashby, M. (1999). *Materials Selection in Mechanical Design*, Butterworth Heinemann editor.
2. Esawi, A. (1994) PhD thesis, Cambridge University.
3. Bassetti, D. (1998) PhD thesis, Institut National Polytechnique de Grenoble.
4. Landru, D. (2000) PhD thesis, Institut National Polytechnique de Grenoble.
5. Granta Design, Cambridge Selection softwares: CMS (1995), CPS (1997), CES (1999).
6. Bassetti, Grenoble, Fuzzymat v3.0 (1997).
7. Landru, D., and Brechet, Y. Grenoble, (1999). CAMD.
8. Ashby, M., and Brechet, Y. *Time Dependant Design* (to be published).
9. Brechet, Y., Ashby, M., and Salvo, L. (2000). *Methodes de choix des materiaux et des procedes*, Presses Universitaires de Lausanne.
10. Ashby, M., (1997). ASTM-STP 1311, 45, *Computerization and Networking of Materials Databases*, Nishijima, S., and Iwata, S., eds.
11. Bassetti, D., Brechet, Y., Heiberg, G., Lingorski, I., Jantzen, A., Pechambert, P., and Salvo, L. (1998). *Materiaux et Techniques* **5**: 31.
12. Deocon, J., Salvo, L., Lemoine, P., Landru, D., Brechet, Y., and Leriche, R. (1999). *Metal Foams and Porous Metal Structures*, Banhardt, J., Ashby, M., and Fleck, N., eds., MIT Verlag Publishing, p. 325.
13. Gibson, L., and Ashby, M. (1999). *Cellular solids*, Cambridge University Press.
14. Pechambert, P., Bassetti, D., Brechet, Y., and Salvo, L. (1996). ICCM7, London IOM, 283.
15. Bassetti, D., Brechet, Y., Heiberg, G., Lingorski, I., Pechambert, P., and Salvo, L. (1998). *Composite Design for Performance*, p. 88, Nicholson, P., ed., Lake Louise.
16. Landru, D., Brechet, Y. (1996). *Colloque Franco espagnol*, p. 41, Yavari, R., ed., Institut National Polytechnique de Grenoble.
17. Landru, D., Ashby, M., and Brechet, Y. *Finding New Applications for a Material* (to be published).
18. Lovatt, A., Bassetti, D., Shercliff, H., and Brechet Y. (1999). *Int. Journal Cast Metals Research* **12**: 211.
19. Heiberg, G., Brechet, Y., Roven, H., and Jensrud, O. *Materials and Design* (in press, 2000).

20. Lebacq, C., Jeggy, T., Brecht, Y., and Salvo, L. (1998). *Materiaux et Techniques* **5**: 39.
21. Lebacq, C., Brechet, Y., Jeggy, T., Salvo, L., and Shercliff, H. (2000). Selection of joining methods. Submitted to *Materials and Design* (see note 19).
22. Landru, D., Esawi, A., Brechet, Y., and Ashby, M. (2000). Selection of surface treatments (to be published).

CHAPTER 1.3

Size Effect on Structural Strength*

ZDENĚK P. BAŽANT
Northwestern University, Evanston, Illinois

Contents

*Thanks to the permission of Springer Verlag, Berlin, this article is reprinted from *Archives of Applied Mechanics* (Ingenieur-Archiv) 69, 703–725. A section on the reverse size effect in buckling of sea ice and shells has been added, and some minor updates have been made. The figures are the same.

The article attempts a broad review of the problem of size effect or scaling of failure, which has recently come to the forefront of attention because of its importance for concrete and geotechnical engineering, geomechanics, and arctic ice engineering, as well as in designing large load-bearing parts made of advanced ceramics and composites, e.g., for aircraft or ships. First the main results of the Weibull statistical theory of random strength are briefly summarized and its applicability and limitations described. In this theory as well as plasticity, elasticity with a strength limit, and linear elastic fracture mechanics (LEFM), the size effect is a simple power law because no characteristic size or length is present. Attention is then focused on the deterministic size effect in quasi-brittle materials which, because of the existence of a non-negligible material length characterizing the size of the fracture process zone, represents the bridging between the simple power-law size effects of plasticity and of LEFM. The energetic theory of quasi-brittle size effect in the bridging region is explained, and then a host of

recent refinements, extensions, and ramifications are discussed. Comments on other types of size effect, including that which might be associated with the fractal geometry of fracture, are also made. The historical development of the size effect theories is outlined, and the recent trends of research are emphasized.

1.3.1 INTRODUCTION

The size effect is a problem of scaling, which is central to every physical theory. In fluid mechanics research, the problem of scaling continuously played a prominent role for over a hundred years. In solid mechanics research, though, the attention to scaling had many interruptions and became intense only during the last decade.

Not surprisingly, the modern studies of nonclassical size effect, begun in the 1970s, were stimulated by the problems of concrete structures, for which there inevitably is a large gap between the scales of large structures (e.g., dams, reactor containments, bridges) and scales of laboratory tests. This gap involves in such structures about one order of magnitude (even in the rare cases when a full-scale test is carried out, it is impossible to acquire a sufficient statistical basis on the full scale).

The question of size effect recently became a crucial consideration in the efforts to use advanced fiber composites and sandwiches for large ship hulls, bulkheads, decks, stacks, and masts, as well as for large load-bearing fuselage panels. The scaling problems are even greater in geotechnical engineering, arctic engineering, and geomechanics. In analyzing the safety of an excavation wall or a tunnel, the risk of a mountain slide, the risk of slip of a fault in the earth crust, or the force exerted on an oil platform in the Arctic by a moving mile-size ice floe, the scale jump from the laboratory spans many orders of magnitude.

In most mechanical and aerospace engineering, on the other hand, the problem of scaling has been less pressing because the structural components can usually be tested at full size. It must be recognized, however, that even in that case the scaling implied by the theory must be correct. Scaling is the most fundamental characteristics of any physical theory. If the scaling properties of a theory are incorrect, the theory itself is incorrect.

The size effect in solid mechanics is understood as the effect of the characteristic structure size (dimension) D on the nominal strength σ_N of structure when geometrically similar structures are compared. The nominal stress (or strength, in case of maximum load) is defined as $\sigma_N = c_N P/bD$ or $c_N P/D^2$ for two- or three-dimensional similarity, respectively; $P =$ load

(or load parameter), b structure thickness, and c_N arbitrary coefficient chosen for convenience (normally $c_N = 1$). So σ_N is not a real stress but a load parameter having the dimension of stress. The definition of D can be arbitrary (e.g., the beam depth or half-depth, the beam span, the diagonal dimension, etc.) because it does not matter for comparing geometrically similar structures.

The basic scaling laws in physics are power laws in terms of D, for which no characteristics size (or length) exists. The classical Weibull [113] theory of statistical size effect caused by randomness of material strength is of this type. During the 1970s it was found that a major deterministic size effect, overwhelming the statistical size effect, can be caused by stress redistributions caused by stable propagation of fracture or damage and the inherent energy release. The law of the deterministic stable effect provides a way of bridging two different power laws applicable in two adjacent size ranges. The structure size at which this bridging transition occurs represents characteristics size.

The material for which this new kind of size effect was identified first, and studied in the greatest depth and with the largest experimental effort by far, is concrete. In general, a size effect that bridges the small-scale power law for nonbrittle (plastic, ductile) behavior and the large-scale power law for brittle behavior signals the presence of a certain non-negligible characteristics length of the material. This length, which represents the quintessential property of quasi-brittle materials, characterizes the typical size of material inhomogeneities or the fracture process zone (FPZ). Aside from concrete, other quasi-brittle materials include rocks, cement mortars, ice (especially sea ice), consolidated snow, tough fiber composites and particulate composites, toughened ceramics, fiber-reinforced concretes, dental cements, bone and cartilage, biological shells, stiff clays, cemented sands, grouted soils, coal, paper, wood, wood particle board, various refractories and filled elastomers, and some special tough metal alloys. Keen interest in the size effect and scaling is now emerging for various "high-tech" applications of these materials.

Quasi-brittle behavior can be attained by creating or enhancing material inhomogeneities. Such behavior is desirable because it endows the structure made from a material incapable of plastic yielding with a significant energy absorption capability. Long ago, civil engineers subconsciously but cleverly engineered concrete structures to achieve and enhance quasi-brittle characteristics. Most modern "high-tech" materials achieve quasi-brittle characteristics in much the same way — by means of inclusions, embedded reinforcement, and intentional microcracking (as in transformation toughening of ceramics, analogous to shrinkage microcracking of concrete). In effect, they emulate concrete.

In materials science, an inverse size effect spanning several orders of magnitude must be tackled in passing from normal laboratory tests of material strength to microelectronic components and micromechanisms. A material that follows linear elastic fracture mechanics (LEFM) on the scale of laboratory specimens of sizes from 1 to 10 cm may exhibit quasi-brittle or even ductile (plastic) failure on the scale of 0.1 to 100 microns.

The purpose of this article is to present a brief review of the basic results and their history. For an in-depth review with several hundred literature references, the recent article by Bažant and Chen [18] may be consulted. A full exposition of most of the material reviewed here is found in the recent book by Bažant and Planas [32], henceforth simply referenced as [BP]. The problem of scale bridging in the micromechanics of materials, e.g., the relation of dislocation theory of continuum plasticity, is beyond the scope of this review (it is treated in this volume by Hutchinson).

1.3.2 HISTORY OF SIZE EFFECT UP TO WEIBULL

Speculations about the size effect can be traced back to Leonardo da Vinci (1500s) [118]. He observed that "among cords of equal thickness the longest is the least strong," and proposed that "a cord is so much stronger as it is shorter," implying inverse proportionality. A century later, Galileo Galilei [64] the inventor of the concept of stress, argued that Leonardo's size effect cannot be true. He further discussed the effect of the size of an animal on the shape of its bones, remarking that bulkiness of bones is the weakness of the giants.

A major idea was spawned by Mariotte [82]. Based on his extensive experiments, he observed that "a long rope and a short one always support the same weight unless that in a long rope there may happen to be some faulty place in which it will break sooner than in a shorter," and proposed the principle of "the inequality of matter whose absolute resistance is less in one place than another." In other words, the larger the structure, the greater is the probability of encountering in it an element of low strength. This is the basic idea of the statistical theory of size effect.

Despite no lack of attention, not much progress was achieved for two and half centuries, until the remarkable work of Griffith [66] the founder of fracture mechanics. He showed experimentally that the nominal strength of glass fibers was raised from 42,300 psi to 491,000 psi when the diameter decreased from 0.0042 in. to 0.00013 in., and concluded that "the weakness of isotropic solids . . . is due to the presence of discontinuities or flaws. . . . The

effective strength of technical materials could be increased 10 or 20 times at least if these flaws could be eliminated." In Griffith's view, however, the flaws or cracks at the moment of failure were still only microscopic; their random distribution controlled the macroscopic strength of the material but did not invalidate the concept of strength. Thus, Griffith discovered the physical basis of Mariotte's statistical idea but not a new kind of size effect.

The statistical theory of size effect began to emerge after Peirce [92] formulated the weakest-link model for a chain and introduced the extreme value statistics which was originated by Tippett [107] and Fréchet [57] and completely described by Fischer and Tippett [58], who derived the Weibull distribution and proved that it represents the distribution of the minimum of any set of very many random variables that have a threshold and approach the threshold asymptotically as a power function of any positive exponent. Refinements were made by von Mises [108] and others (see also [62, 63, 103, 56]. The capstone of the statistical theory of strength was laid by Weibull [113] (also [114–116]). On a heuristic and experimental basis, he concluded that the tail distribution of low strength values with an extremely small probability could not be adequately represented by any of the previously known distributions and assumed the cumulative probability distribution of the strength of a small material element to be a power function of the strength difference form a finite or zero threshold. The resulting distribution of minimum strength, which was the same as that derived by Fischer and Tippet [58] in a completely different context, came to be known as the Weibull distribution. Others [62, 103] later offered a theoretical justification by means of a statistical distribution of microscopic flaws or microcracks. Refinements and applications to metals and ceramics (fatigue embrittlement, cleavage toughness of steels at a low and brittle-ductile transition temperatures, evaluation of scatter of fracture toughness data) have continued until today [37, 56, 77, 101]. Applications of Weibull's theory to fatigue embrittled metals and to ceramics have been researched thoroughly [75, 76]. Applications to concrete, where the size effect has been of the greatest concern, have been studied by Zaitsev and Wittmann [122], Mihashi and Izumi [88], Wittmann and Zaitsev [121], Zech and Wittmann [123], Mihashi [84], Mihashi and Izumi [85] Carpinteri [41, 42], and others.

Until about 1985, most mechanicians paid almost no attention to the possibility of a deterministic size effect. Whenever a size effect was detected in tests, it was automatically assumed to be statistical, and thus its study was supposed to belong to statisticians rather than mechanicians. The reason probably was that no size effect is exhibited by the classical continuum mechanics in which the failure criterion is written in terms of stresses and strains (elasticity with strength limit, plasticity and viscoplasticity, as well as fracture mechanics of bodies containing only microscopic cracks or

flaws) [8]. The subject was not even mentioned by S. P. Timoshenko in 1953 in his monumental *History of the Strength of Materials*.

The attitude, however, changed drastically in the 1980s. In consequence of the well-funded research in concrete structures for nuclear power plants, theories exhibiting a deterministic size effect have developed. We will discuss it later.

1.3.3 POWER SCALING AND THE CASE OF NO SIZE EFFECT

It is proper to explain first the simple scaling applicable to all physical systems that involve no characteristic length. Let us consider geometrically similar systems, for example, the beams shown in Figure 1.3.1a, and seek to deduce the response Y (e.g., the maximum stress or the maximum deflection) as a function of the characteristic size (dimension) D of the structure; $Y = Y_0 f(D)$

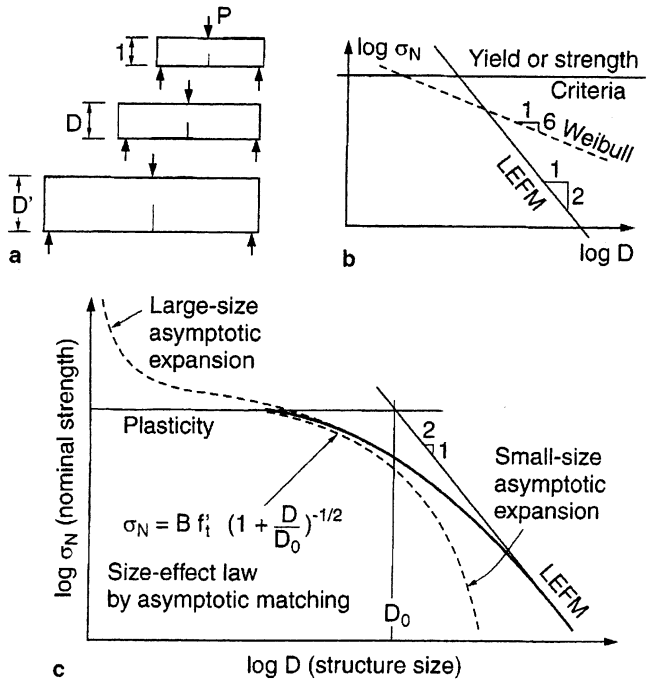

FIGURE 1.3.1 a. Top left: Geometrically similar structures of different sizes. b. Top right: Power scaling laws. c. Bottom. Size effect law for quasi-brittle failures bridging the power law of plasticity (horizontal asymptote) and the power law of LEFM (inclined asymptote).

where u is the chosen unit of measurement (e.g., 1 m, 1 mm). We imagine three structure sizes 1, D, and D' (Figure 1.3.1a). If we take size 1 as the reference size, the responses for sizes D and D' are $Y = f(D)$ and $Y' = f(D')$. However, since there is no characteristic length, we can also take size D as the reference size. Consequently, the equation

$$f(D')/f(D) = f(D'/D) \tag{1}$$

must hold ([8, 18]; for fluid mechanics [2, 102]). This is a functional equation for the unknown scaling law $f(D)$. It has one and only one solution, namely, the power law:

$$f(D) = (D/c_1)^s \tag{2}$$

where $s =$ constant and c_1 is a constant which is always implied as a unit of length measurement (e.g., 1 m, 1 mm). Note that c_1 cancels out of Eq. 2 when the power function (Eq. 1) is substituted.

On the other hand, when, for instance, $f(D) = \log(D/c_1)$, Eq. 1 is not satisfied and the unit of measurement, c_1, does not cancel out. So, the logarithmic scaling could be possible only if the system possessed a characteristic length related to c_1.

The power scaling must apply for every physical theory in which there is no characteristic length. In solid mechanics such failure theories include elasticity with a strength limit, elastoplasticity, and viscoplasticity, as well as LEFM (for which the FPZ is assumed shrunken into a point).

To determine exponent s, the failure criterion of the material must be taken into account. For elasticity with a strength limit (strength theory), or plasticity (or elastoplasticity) with a yield surface expressed in terms of stresses or strains, or both, one finds that $s = 0$ when response Y represents the stress or strain (for example, the maximum stress, or the stress at certain homologous points, or the nominal stress at failure) [8]. Thus, if there is no characteristic dimension, all geometrically similar structures of different sizes must fail at the same nominal stress. By convention, this came to be known as the case of *no size effect*.

In LEFM, on the other hand, $s = -1/2$, provided that the geometrically similar structures with geometrically similar cracks or notches are considered. This may be generally demonstrated with the help of Rice's J-integral [8].

If log σ_N is plotted versus log D, the power law is a straight line (Figure 1.3.1b). For plasticity, or elasticity with a strength limit, the exponent of the power law vanishes, i.e., the slope of this line is 0, while for LEFM the slope is $-1/2$ [8]. An emerging "hot" subject is the quasi-brittle materials and structures, for which the size effect bridges these two power laws.

It is interesting to note that critical stress for elastic buckling of beams, frames, and plates exhibits also no size effect, i.e., is the same for

geometrically similar structures of different sizes. However, this is not true for beams on elastic foundation and for shells [16].

1.3.4 WEIBULL STATISTICAL SIZE EFFECT

The classical theory of size effect has been statistical. Three-dimensional continuous generalization of the weakest link model for the failure of a chain of links of random strength (Fig. 1.3.2a) leads to the distribution

$$P_f(\sigma_N) = 1 - \exp\left[-\int_V c[\boldsymbol{\sigma}(\boldsymbol{\chi}),\ \sigma_N)]dV(\boldsymbol{\chi})\right]s$$

which represents the probability that a structure that fails as soon as macroscopic fracture initiates from a microcrack (or a some flaw) somewhere in the structure; σ = stress tensor field just before failure, $\boldsymbol{\chi}$ = coordinate vector, V = volume of structure, and $c(\boldsymbol{\sigma})$ =function giving the spatial concentration of failure probability of material (= $V_r^{-1} \times$ failure probability of material representative volume V_r) [62]; $c(\boldsymbol{\sigma}) \approx \sum_i P_1(\sigma_i)/V_0$ where σ_i= principal stresses ($i = 1, 2, 3$) and $P_1(\sigma)$= failure probability (cumulative) of the smallest possible test specimen of volume V_0 (or representative

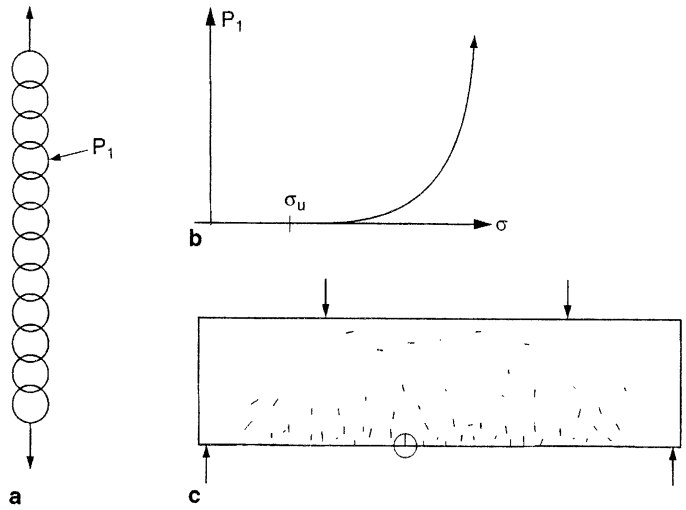

FIGURE 1.3.2 a. Left: Chain with many links of random strength. b. Right top: Failure probability of a small element. c. Right bottom: Structures with many microcracks of different probabilities to become critical.

volume of the material) subject to uniaxial tensile stress σ;

$$P_1(\sigma) = \left\langle \frac{\sigma - \sigma_u}{s_0} \right\rangle^m \tag{4}$$

[113] where m, s_0, σ_1 = material constants (m = Weibull modulus, usually between 5 and 50; s_0 = scale parameter; σ_u = strength threshold, which may usually be taken as 0) and V_0 = reference volume understood as the volume of specimens on which $c(\sigma)$ was measured. For specimens under uniform uniaxial stress (and $\sigma_u = 0$), Eqs. 3 and 4 lead to the following simple expressions for the mean and coefficient of variation of the nominal strength:

$$\begin{aligned} \bar{\sigma}_N &= s_0 \Gamma(1 + m^{-1})(V_0/V)^{1/m} \\ \omega &= [\Gamma(1 + 2m^{-1})/\Gamma^2(1 + m^{-1}) - 1]^{1/2} \end{aligned} \tag{5}$$

where Γ is the gamma function. Since ω depends only on m, it is often used for determining m form the observed statistical scatter of strength of identical test specimens. The expression for $\bar{\sigma}_N$ includes the effect of volume V which depends on size D. In general, for structures with nonuniform multi-dimensional stress, the size effect of Weibull theory (for $\sigma_r \approx 0$) is of the type

$$\bar{\sigma}_N \propto D^{-n_d/m} \tag{6}$$

where $n_d = 1$, 2, or 3 for uni-, two- or three-dimensional similarity.

In view of Eq. 5, the value $\sigma_W = \sigma_N (V/V_0)^{1/m}$ for a uniformity stressed specimen can be adopted as a size-independent stress measure called the Weibull stress. Taking this viewpoint, Beremin [37] proposed taking into account the nonuniform stress in a large crack-tip plastic zone by the so-called Weibull stress:

$$\sigma_W = \left(\sum_i \sigma_{I_i}^m \frac{V_i}{V_0} \right)^{1/m} \tag{7}$$

where V_i ($i = 1, 2, \ldots N_W$) are elements of the plastic zone having maximum principal stress σ_{Ii}. Ruggieri and Dodds [101] replaced the sum in Eq. 5 by an integral; see also Lei *et al.* [77]. Equation 7, however, considers only the crack-tip plastic zone whose size which is almost independent of D. Consequently, Eq. 7 is applicable only if the crack at the moment of failure is not yet macroscopic, still being negligible compared to structural dimensions.

As far as quasi-brittle structures are concerned, applications of the classic Weibull theory face a number of serious objections:

1. The fact that in Eq. 6 the size effect is a power law implies the absence of any characteristic length. But this cannot be true if the material contains sizable inhomogeneities.

2. The energy release due to stress redistributions caused by macroscopic FPZ or stable crack growth before $P_{\max}$ gives rise to a deterministic size effect which is ignored. Thus the Weibull theory is valid only if the structure fails as soon as a microscopic crack becomes macroscopic.
3. Every structure is mathematically equivalent to a uniaxially stressed bar (or chain, Fig. 1.3.2), which means that no information on the structural geometry and failure mechanism is taken into account.
4. The size effect differences between two- and three-dimensional similarity ($n_d = 2$ or 3) are predicted much too large.
5. Many tests of quasi-brittle materials (e.g., diagonal shear failure of reinforced concrete beams) show a much stronger size effect than predicted by the Weibull theory ([BP]), and the review in Bažant [9]).
6. The classical theory neglects the spatial correlations of material failure probabilities of neighboring elements caused by nonlocal properties of damage evolution (while generalizations based on some phenomenological load-sharing hypotheses have been divorced from mechanics).
7. When Eq. 5 is fitted to the test data on statistical scatter for specimens of one size ($V = \text{const.}$) and when Eq. 6 is fitted to the mean test data on the effect of size or V (of unnotched plain concrete specimens), the optimum values of Weibull exponent m are very different, namely, $m = 12$ and $m = 24$, respectively. If the theory were applicable, these values would have to coincide.

In view of these limitations, among concrete structures Weibull theory appears applicable to some extremely thick plain (unreinforced) structures, e.g., the flexure of an arch dam acting as a horizontal beam (but not for vertical bending of arch dams or gravity dams because large vertical compressive stresses cause long cracks to grow stably before the maximum load). Most other plain concrete structures are not thick enough to prevent the deterministic size effect from dominating. Steel or fiber reinforcement prevents it as well.

1.3.5 QUASI-BRITTLE SIZE EFFECT BRIDGING PLASTICITY AND LEFM, AND ITS HISTORY

Qausi-brittle materials are those that obey on a small scale the theory of plasticity (or strength theory), characterized by material strength or yield limit σ_0, and on a large scale the LEFM, characterized by fracture energy G_f. While plasticity alone, as well as LEFM alone, possesses no characteristics length, the combination of both, which must be considered for the bridging of plasticity and LEFM, does. Combination of σ_0 and G_f yields Irwin's (1958)

characteristic length (material length):

$$\ell_0 = \frac{EG_f}{\sigma_0^2} \tag{8}$$

which approximately characterizes the size of the FPZ (E = Young's elastic modulus). So the key to the deterministic quasi-brittle size effect is a combination of the concept of strength or yield with fracture mechanics. In dynamics, this further implies the existence of a characteristic time (material time):

$$\tau_0 = \ell_0/v \tag{9}$$

representing the time a wave of velocity v takes to propagate the distance ℓ_0.

After LEFM was first applied to concrete [72], it was found to disagree with test results [74, 78, 111, 112]. Leicester [78] tested geometrically similar notched beams of different sizes, fitted the results by a power law, $\sigma_N \propto D^{-n}$, and observed that the optimum n was less than 1/2, the value required by LEFM. The power law with a reduced exponent of course fits the test data in the central part of the transitional size range well but does not provide the bridging of the ductile and LEFM size effects. An attempt was made to explain the reduced exponent value by notches of a finite angle, which, however, is objectionable for two reasons: (i) notches of a finite angle cannot propagate (rather, a crack must emanate from the notch tip), and (ii) the singular stress field of finite-angle notches gives a zero flux of energy into the notch tip. Like Weibull theory, Leicester's power law also implied the nonexistence of a characteristic length (see Bažant and Chen [18], Eqs. 1–3), which cannot be the case for concrete because of the large size of its inhomogeneities. More extensive tests of notched geometrically similar concrete beams of different sizes were carried out by Walsh [111, 112]. Although he did not attempt a mathematical formulation, he was first to make the doubly logarithmic plot of nominal strength versus size and observe that it is was transitional between plasticity and LEFM.

An important advance was made by Hillerborg *et al*. [68] (also Peterson [93]). Inspired by the softening and plastic FPZ models of Barenblatt [2, 3] and Dugdale [55], they formulated the cohesive (or fictitious) crack model characterized by a softening stress-displacement law for the crack opening and showed by finite element calculations that the failures of unnotched plain concrete beams in bending exhibit a deterministic size effect, in agreement with tests of the modulus of rupture.

Analyzing distributed (smeared) cracking damage, Bažant [4] demonstrated that its localization into a crack band engenders a deterministic size effect on the postpeak deflections and energy dissipation of structures. The effect of the crack band is approximately equivalent to that of a long fracture

with a sizable FPZ at the tip. Subsequently, using an approximate energy release analysis, Bažant [5] derived for the quasi-brittle size effect in structures failing after large stable crack growth the following approximate size effect law:

$$\sigma_N = B\sigma_0\left(1+\frac{D}{D_0}\right)^{-1/2}+\sigma_R \tag{10}$$

$$\text{or more generally:}\quad \sigma_N = B\sigma_0\left[1+\left(\frac{D}{D_0}\right)^{r}\right]^{-1/2r}+\sigma_R \tag{11}$$

in which r, B = positive dimensionless constants; D_0 = constant representing the transitional size (at which the power laws of plasticity and LEFM intersect); and D_0 and B characterize the structure geometry. Usually constant $\sigma_R = 0$, except when there is a residual crack-bridging stress σ_r outside the FPZ (as in fiber composites), or when at large sizes some plastic mechanism acting in parallel emerges and becomes dominant (as in the Brazilian split-cylinder test).

Equation 10 was shown to be closely followed by the numerical results for the crack band model [4, 30] as well as for the nonlocal continuum damage models, which are capable of realistically simulating the localization of strain-softening damage and avoiding spurious mesh sensitivity; see the article on Stability in this volume.

Beginning in the mid-1980s, the interest in the quasi-brittle size effect of concrete structures surged enormously and many researchers made noteworthy contributions, including Planas and Elices [94–96], Petersson [93], and Carpinteri [41]. The size effect has recently become a major theme at conferences on concrete fracture [7, 35, 86, 87, 120].

Measurements of the size effect on $P_{\max}$ were shown to offer a simple way to determine the fracture characteristics of quasi-brittle materials, including the fracture energy, the effective FPZ length, and the (geometry dependent) R-curve.

1.3.6 SIZE EFFECT MECHANISM: STRESS REDISTRIBUTION AND ENERGY RELEASE

Let us now describe the gist of the deterministic quasi-brittle size effect. LEFM applies when the FPZ is negligibly small compared to structural dimension D and can be considered as a point. Thus the LEFM solutions can be obtained by methods of elasticity. The salient characteristic of quasi-brittle materials is that there exists a sizable FPZ with distributed cracking or other

softening damage that is not negligibly small compared to structural dimension D. This makes the problem nonlinear, although approximately equivalent LEFM solutions can be applied unless FPZ reaches near the structure boundaries.

The existence of a large FPZ means that the distance between the tip of the actual (traction-free) crack and the tip of the equivalent LEFM crack at $P_{\max}$ is equal to a certain characteristics length c_f (roughly one half of the FPZ size) that is not negligible compared to D. This causes a non-negligible macroscopic stress redistribution with energy release from the structure.

With respect to the fracture length a_0 (distance from the mouth of notch or crack to the beginning of the FPZ), two basic cases may now be distinguished: (i) $a_0 = 0$, which means that $P_{\max}$ occurs at the initiation of macroscopic fracture propagation, and (ii) a_0 is finite and not negligible compared to D, which means that $P_{\max}$ occurs after large stable fracture growth.

1.3.6.1 Scaling for Failure at Crack Initiation

An example of the first case is the modulus of rupture test, which consists in the bending of a simply supported beam of span L with a rectangular cross section of depth D and width b, subjected to concentrated load P; the maximum load is not decided by the stress $\sigma_1 = 3PL/2bD^2$ at the tensile face, but by the stress value $\bar{\sigma}$ roughly at distance $c_f/2$ from the tensile face (which is at the middle of FPZ). Because $\bar{\sigma} = \sigma_1 - \sigma_1' c_f/2$ where $\sigma_1' =$ stress gradient $= 2\sigma_1/D$, and also because $\bar{\sigma} = \sigma =$ intrinsic tensile strength of the material, the failure condition $\bar{\sigma} = \sigma_0$ yields $P/bD = \sigma_N = \sigma_0/(1 - D_b/D)$ where $D_b = (3L/2D)c_f$, which is a constant because for geometrically similar beams $L/D =$ constant. This expression, however, is unacceptable for $D \leq D_b$. But since the derivation is valid only for small enough c_f/D, one may replace it by the following asymptotically equivalent size effect formula:

$$\sigma_N = \sigma_0 \left(1 + \frac{rD_b}{D}\right)^{1/r} \tag{12}$$

which happens to be acceptable for the whole range of D (including $D \to 0$); r is any positive constant. The values $r = 1$ or 2 have been used for concrete [12], while $r \approx 1.45$ is optimum according to Bažant and Novák's latest analysis of test data at Northwestern University (yet unpublished).

1.3.6.2 Scaling for Failures with a Long Crack or Notch

Let us now give a simple explanation of the second case of structures failing only after stable formation of large cracks, or notched fracture specimens. Failures of this type, exhibiting a strong size effect ([BP], [21, 65, 69, 83, 104, 110]) are typical of reinforced concrete structures or fiber composites [119], and are also exhibited by some unreinforced structures (e.g., dams, due to the effect of vertical compression, or floating ice plates in the Arctic). Consider the rectangular panel in Fig. 1.3.3, which is initially under a uniform stress equal to σ_N. Introduction of a crack of length a with a FPZ of a certain length and width h may be approximately imagined to relieve the stress, and thus release the strain energy, from the shaded triangles on the flanks of the crack band shown in Figure 1.3.3. The slope k of the effective boundary of the stress relief zone need not be determined; what is important is that k is independent of the size D.

For the usual ranges of interest, the length of the crack at maximum load may normally be assumed approximately proportional to the structure size D, while the size h of the FPZ is essentially a constant, related to the inhomogeneity size in the material. This has been verified for many cases by experiments (showing similar failure modes for small and large specimens) and finite element solutions based on crack band, cohesive, or nonlocal models.

The stress reduction in the triangular zones of areas $ka^2/2$ (Fig. 1.3.3) causes (for the case $b = 1$) the energy release $U_a = 2\times(ka^2/2)\sigma_N^2/2E$. The stress drop within the crack band of width h causes further energy release

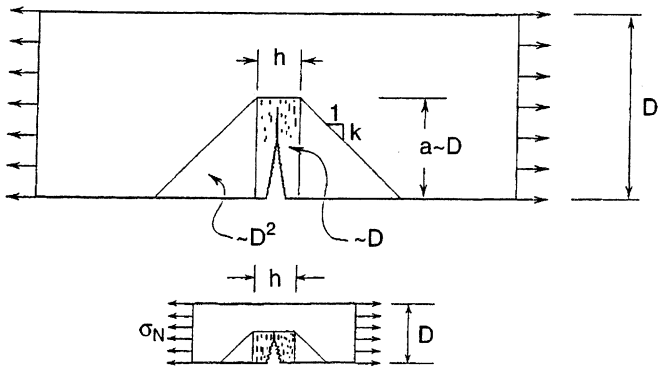

FIGURE 1.3.3 Approximate zones of stress relief due to fracture.

$U_b = ha\sigma_N^2/E$. The total energy dissipated by the fracture is $W = aG_f$, where G_f is the fracture energy, a material property representing the energy dissipated per unit area of the fracture surface. Energy balance during static failure requires that $\partial(U_a + U_b)/\partial a = dW/da$. Setting $a = D(a/D)$ where a/D is approximately a constant if the failures for different structure sizes are geometrically similar, the solution of the last equation for $gma;_N$ yields Bažant's [5] approximate size effect law in Eq. 10 with $\sigma_R = 0$ (Fig. 1.3.1c).

More rigorous derivations of this law, applicable to arbitrary structure geometry, have been given in terms of asymptotic analysis–based equivalent LEFM [10] or on Rice's path-independent J-integral [32]. This law has also been verified by nonlocal finite element analysis and by random particle (or discrete element) models. The experimental verifications, among which the earliest is found in the famous Walsh's [111, 112] tests of notched concrete beams, have by now become abundant (e.g., Fig. 1.3.4).

For very large sizes ($D \gg D_0$), the size effect law in Eq. 10 reduces to the power law $\sigma_N \propto D^{-1/2}$, which represents the size effect of LEFM (for geometrically similar large cracks) and corresponds to the inclined asymptote of slope $-1/2$ in Figure 1.3.1c. For very small sizes ($D \ll D_0$), this law reduces to $\sigma_N =$ constant, which corresponds to the horizontal asymptote and means that there is no size effect, as in plastic limit analysis.

The ratio $\beta = D/D_0$ is called the brittleness number of a structure. For $\beta \to \infty$ the structure is perfectly brittle (i.e., follows LEFM), in which case the size effect is the strongest possible, while for $\beta \to 0$ the structure is nonbrittle (or ductile, plastic), in which case there is no size effect. Quasi-brittle structures are those for which $0.1 \leq \beta \leq 10$, in which case the size effect represents a smooth transition (or interpolation) that bridges the power law size effects for the two asymptotic cases. The law (Eq. 10) has the character of asymptotic matching and serves to provide the bridging of scales. In the quasi-brittle range, the stress analysis is of course nonlinear, calling for the cohesive crack model or the crack band model (which are mutually almost equivalent), or some of the nonlocal damage models.

The meaning of the term quasi-brittle is relative. If the size of a quasi-brittle structure becomes sufficiently large compared to material inhomogeneities, the structure becomes perfectly brittle (for concrete structures, only the global fracture of a large dam is describable by LEFM), and if the size becomes sufficiently small, the structure becomes nonbrittle (plastic, ductile) because the FPZ extends over the whole cross section of the structure (thus a micromachine or a miniature electronic device made of silicone or fine-grained ceramic may be quasi-brittle or nonbrittle).

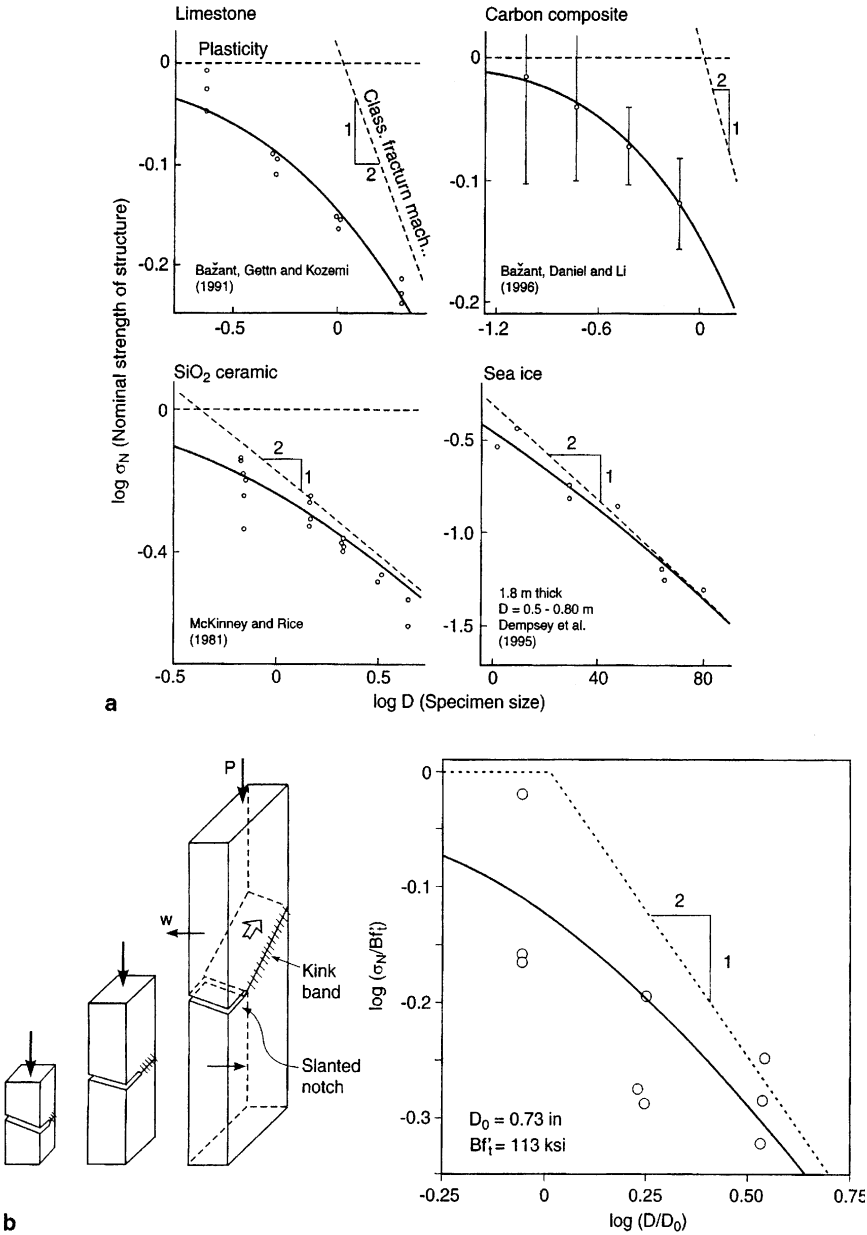

FIGURE 1.3.4 Top: Comparisons of size effect law with Mode 1 test data obtained by various investigators using notched specimens of different materials. Bottom: Size effect in compression kink-band failures of geometrically similar notched carbon-PEEK specimens [ ].

1.3.6.3 Size Effect on Postpeak Softening and Ductility

The plots of nominal stress versus the relative structure deflection (normalized so as to make the initial slope in Figure 1.3.5 size-independent) have, for small and large structures, the shapes indicated in Figure 1.3.5. Apart from the size effect on P_{max}, there is also a size effect on the shape of the postpeak descending load-deflection curve. For small structures the postpeak curves descend slowly, for larger structures steeper, and for sufficiently large structures they may exhibit a snapback, that is, a change of slope from negative to positive.

If a structure is loaded under displacement control through an elastic device with spring constant C_s, it loses stability and fails at the point where the load-deflection diagram first attains the slope $-C_s$ (if ever); Figure 1.3.5. The ratio of the deflection at these points to the elastic deflection characterizes the ductility of the structure. As is apparent from the figure,

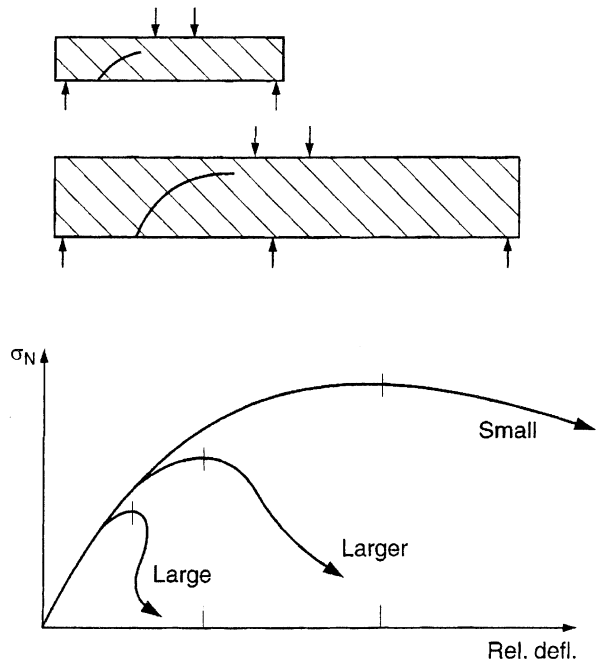

FIGURE 1.3.5 Load-deflection curves of quasi-brittle structures of different sizes, scaled to the same initial slope.

small quasi-brittle structures have a large ductility, whereas large quasi-brittle structures have small ductility.

The areas under the load-deflection curves in Figure 1.3.5 characterize the energy absorption. The capability of a quasi-brittle structure to absorb energy decreases, in relative terms, as the structure size increases. The size effect on energy absorption capability is important for blast loads and impact.

The progressive steepening of the postpeak curves in Figure 1.3.5 with increasing size and the development of a snapback can be most simply described by the series coupling model, which assumes that the response of a structure may be at least approximately modeled by the series coupling of the cohesive crack or damage zone with a spring characterizing the elastic unloading of the rest of the structure (Bažant and Cedolin [17], Sec. 13.2).

1.3.6.4 Asymptotic Analysis of Size Effect by Equivalent LEFM

To obtain simple approximate size effect formulae that give a complete prediction of the failure load, including the effect of geometrical shape of the structure, equivalent LEFM may be used. In this approach the tip of the equivalent LEFM (sharp) crack is assumed to lie approximately a distance c_f ahead of the tip of the traction-free crack or notch, c_f being a constant (representing roughly one half of the length of the FPZ ahead of the tip. Two cases are relatively simple: (i) If a large crack grows stably prior to $P_{\max}$ or if there is a long notch,

$$\sigma_N = \frac{\sqrt{EG_f} + \sigma_Y\sqrt{\gamma'(\alpha_0)c_f + \gamma(\alpha_0)D}}{\sqrt{g'(\alpha_0)c_f + g(\alpha_0)D}} \tag{13}$$

and (ii) if $P_{\max}$ occurs at fracture initiation from a smooth surface

$$\sigma_N = \frac{\sqrt{EG_f} + \sigma_Y\sqrt{\gamma'(0)c_f + \gamma''(0)(c_f^2/2D)}}{\sqrt{g'(0)c_f + g''(0)(c_f^2/2D)}} \tag{14}$$

[10, 12] where the primes denote derivatives; $g(\alpha_0) = K_{IP}^2/\sigma_N^2 D$ and $\gamma(\alpha_0) = K_{I\sigma}^2/\sigma_Y^2 D$ are dimensionless energy release functions of LEFM of $\alpha = a_0/D$ where a_0 = length of notch or crack up to the beginning of the FPZ; K_{IP}, $K_{I\sigma}$ = stress intensity factors for load P and for loading by uniform residual crack-bridging stress σ_Y, respectively; $\sigma_Y > 0$ for tensile fracture, but $\sigma_Y \neq 0$ in the case of compression fracture in concrete, kink band propagation in fiber composites, and tensile fracture of composites reinforced by fibers short

enough to undergo frictional pullout rather than breakage. The asymptotic behavior of Eq. 13 for $D \to \infty$ is of the LEFM type, $\sigma_N - \sigma_Y \propto D^{-1/2}$. Equation 14 approaches for $D \to \infty$ a finite asymptotic value. So does Eq. 13 if $\sigma_Y > 0$.

1.3.6.5 Size Effect Method for Measuring Material Constants and R-Curve

Comparison of Eq. 13 with Eq. 10 yields the relations:

$$D_0 = c_f g'(\alpha_0)/g(\alpha_0) \qquad B\sigma_0 = \sigma_0 \sqrt{EG_f/c_f g'(\alpha_0)} \tag{15}$$

Therefore, by fitting Eq. 10 with $\sigma_R = 0$ to the values of σ_N measured on test specimens of different sizes with a sufficiently broad range of brittleness numbers $\beta = D/D_0$, the values of G_f and c_f can be identified [20, 31]. The fitting can be best done by using the Levenberg-Marquardt nonlinear optimization algorithm, but it can also be accomplished by a (properly weighted) linear regression of σ_N^{-2} versus D. The specimens do not have to be geometrically similar, although when they are the evaluation is simpler and the error smaller. The lower the scatter of test results, the narrower is the minimum necessary range of β (for concrete and fiber composites, the size range 1:4 is the minimum).

The size effect method of measuring fracture characteristics has been adopted for an international standard recommendation for concrete ([99], [BP] Sec. 6.3), and has also been verified and used for various rocks, ceramics, orthotropic fiber-polymer composites, sea ice, wood, tough metals, and other quasi-brittle materials. The advantage of the size effect method is that the tests, requiring only the maximum loads, are foolproof and easy to carry out. With regard to the cohesive crack model, note that the size effect method gives the energy value corresponding to the area under the initial tangent of the softening stress-displacement curve, rather than the total area under the curve.

The size effect method also permits determining the R-curve (resistance curve) of the quasi-brittle material — a curve that represents the apparent variation of fracture energy with crack extension for which LEFM becomes approximately equivalent to the actual material with a large FPZ. The R-curve, which (in contrast to the classical R-curve definition) depends on the specimen geometry, can be obtained as the envelope of the curves of the energy release rate at $P = P_{\max}$ (for each size) versus the crack extension for specimens of various sizes. In general, this can easily be done numerically,

and if the size effect law has the form in Eq. 10 with $\sigma_R = 0$, a parametric analytical expression for the R-curve exists ([20], [BP] Sec. 6.4).

The fracture model implied by the size effect law in Eq. 10 or Eq. 13 has one independent characteristic length, c_f, representing about one half of the FPZ length. Because of Eq. 15, the value of ℓ_0 is implied by c_f if σ_0 is known. The value of c_f controls the size D_0 at the center of the bridging region (intersection of the power-law asymptotes in Figure 1.3.1c, and σ_0 or G_f controls a vertical shift of the size effect curve at constant D_0. The location of the large-size asymptote depends only on K_c and geometry, and the location of the small-size asymptote depends only on σ_0 and geometry.

1.3.6.6 Critical Crack-Tip Opening Displacement, δ_{CTOD}

The quasi-brittle size effect, bridging plasticity and LEFM, can also be simulated by the fracture models characterized by the critical stress intensity factor K_c (fracture toughness) and δ_{CTOD}; for metals see Wells [117] and Cottrell [50], and for concrete Jenq and Shah [70]. Jenq and Shah's model, called the two-parameter fracture model, has been shown to give essentially the same results as the R-curve derived from the size effect law in Eq. 10 with $\sigma_R = 0$. The models are in practice equivalent because

$$K_c = \sqrt{EG_f} \qquad \delta_{CTOD} = (1/\pi)\sqrt{8G_f c_f/E} \tag{16}$$

Using these formulae, the values of K_c and δ_{CTOD} can be easily identified by fitting the size effect law (Eq. 10) to measured $P_{\max}$ value.

Like the size effect law in Eq. 10 with $\sigma_R = 0$, the two-parameter model has only one independent characteristic length, $\ell_0 = K_c^2/\sigma_0^2$. If σ_0 is known, then δ_{CTOD} is not an independent length because c_f is implied by ℓ_0 and δ_{CTOD} then follows from Eq. 16.

1.3.7 EXTENSIONS, RAMIFICATIONS, AND APPLICATIONS

1.3.7.1 Size Effects in Compression Fracture

Loading by high compressive stress without sufficient lateral confining stresses leads to damage in the form of axial splitting microcracks engendered

by pores, inclusions, or inclined slip planes. This damage localizes into a band that propagates either axially or laterally.

For axial propagation, the energy release from the band drives the formation of the axial splitting fracture, and since this energy is proportional to the length of the band, there is no size effect. For lateral propagation, the stress in the zones on the sides of the damage band gets reduced, which causes an energy release that grows in proportion to D^2, while the energy consumed and dissipated in the band grows in proportion to D. The mismatch of energy release rates inevitably engenders a deterministic size effect of the quasi-brittle type, analogous to the size effect associated with tensile fracture. In consequence of the size effect, failure by lateral propagation must prevail over the failure by axial propagation if a certain critical size is exceeded.

The size effect can again be approximately described by the equivalent LEFM. This leads to Eq. 13 in which σ_Y is determined by analysis of the microbuckling in the laterally propagating band of axial splitting cracks. The spacing s of these cracks is in Eq. 13 assumed to be dictated by material inhomogeneities. However, if the spacing is not dictated and is such that it minimizes σ_N, then the size effect gets modified as

$$\sigma_N = CD^{-2/5} + \sigma_\infty \tag{17}$$

([BP] Sec. 10.5.11) where C, σ_∞ = constants, the approximate values of which have been calculated for the breakout of boreholes in rock.

1.3.7.2 Fracturing Truss Model for Concrete and Boreholes in Rock

Propagation of compression fracture is what appears to control maximum load in diagonal shear failure of reinforced concrete beams with or without stirrups, for which a very strong size effect has been demonstrated experimentally [9, 21, 69, 71, 91, 98, 104, 109, 110]. A long diagonal tension crack grows stably under shear loading until the concrete near its tip gets crushed. A simplified formula for the size effect can be obtained by energetic modification of the classical truss model (strut-and-tie model) [9].

The explosive breakout of boreholes (or mining stopes) in rock under very high pressures is known to also exhibit size effect, as revealed by the tests of Carter [47], Carter *et al.* [48], Haimson and Herrick [67], and Nesetova and Lajtai [90]. An approximate analytical solution can be obtained by exploiting Eschelby's theorem for eigenstresses in elliptical inclusions [27].

1.3.7.3 Kink Bands in Fiber Composites

A link band, in which axial shear-splitting cracks develop between fibers which undergo microbuckling, is one typical mode of compression failure of composites or laminates with uniaxial fiber reinforcement. This failure mode, whose theory was begun by Rosen [100] and Argon [1], was until recently treated by the theory of plasticity, which implies no size effect. Recent experimental and theoretical studies [40], however, revealed that the kink band propagates sideway like a crack and the stress on the flanks of the band gets reduced to a certain residual value, which is here denoted as σ_Y and can be estimated by the classical plasticity approach of Budiansky [39]. The cracklike behavior implies a size effect, which is demonstrated by the latest Bažant *et al*. [22, 24] laboratory tests of notched carbon-PEEK specimens (Fig. 1.3.4); these tests also demonstrated the possibility of a stable growth of a long kink band, which was achieved by rotational restraint at the ends).

There are again two types of size effect, depending on whether $P_{\max}$ is reached (i) when the FPZ of the kink band is attached to a smooth surface or (ii) or when there exists either a notch or a long segment of kink band in which the stress has been reduced to σ_Y. Equations 13 and 14, respectively, approximately describe the size effects for these two basic cases; in this case G_f now plays the role of fracture energy of the kink band (area below the stress-contraction curve of the kink bank and above the σ_Y value), and c_f the role of the FPZ of the kink band, which is assumed to be approximately constant, governed by material properties.

The aforementioned carbon-PEEK tests also confirm that case (ii), in which a long kink band grows stably prior to $P_{\max}$, is possible (in those tests, this is by virtue of a lateral shift of compression resultant in wide notched prismatic specimens with ends restrained against rotation).

1.3.7.4 Size Effects in Sea Ice

Normal laboratory specimens of sea ice exhibit no notch sensitivity. Therefore, failure of sea ice has been thought to be well described by plastic limit analysis, which exhibits no size effect [73, 106]. This perception, however, changed drastically after Dempsey carried out in 1993 on the Arctic Ocean size effect tests of floating notched square specimens with an unprecedented, record-breaking size range (with square sides ranging from 0.5 m to 80 m!) [52, 53, 89].

It is now clear that floating sea ice plates are quasi-brittle and their size effect on the scale of 100 m approaches that of LEFM. Among other things,

Dempsey's major experimental result explains why the measured forces exerted by moving ice on a fixed oil platform are one to two orders of magnitude smaller than the predictions of plastic limit analysis based on the laboratory strength of ice. The size effect law in Eq. 10 with $\sigma_R = 0$, or in Eq. 13 (with $\sigma_Y = 0$), agree with these results well, permitting the values of G_f and c_f of sea ice to be extracted by linear regression of the $P_{\max}$ data. The value of c_f is in the order of meters (which can be explained by inhomogeneities such as brine pockets and channels, as well as preexisting thermal cracks, bottom roughness of the plate, warm and cold spots due to alternating snow drifts, etc.). Information on the size effect in sea ice can also be extracted from acoustic measurements [80].

Rapid cooling in the Arctic can produce in the floating plate bending moments large enough to cause fracture. According to plasticity or elasticity with a strength limit, the critical temperature difference ΔT_{cr} across the plate would have to be independent of plate thickness D. Fracture analysis, however, indicated a quasi-brittle size effect. Curiously, its asymptotic form is not $\Delta T_{cr} \propto D^{-1/2}$ but

$$\Delta T_{cr} \propto D^{-3/8} \tag{18}$$

[10]. The reason is that D is not a characteristic dimension in the plane of the boundary value problem of plate bending; rather, it is the flexural wavelength of a plate on elastic foundation, which is proportional to $D^{4/3}$ rather than D. It seems that Eq. 18 may explain why long cracks of length 10 to 100 km, which suddenly form in the fall in the Arctic ice cover, often run through thick ice floes and do not follow the thinly refrozen water leads around the floes.

In analyzing the vertical penetration of floating ice plate (load capacity for heavy objects on ice, or the maximum force P required for penetration from below), one must take into account that bending cracks are reached only through part of the thickness, their ligaments transmitting compressive forces, which produces a dome effect. Because at maximum load that part-through bending crack (of variable depth profile) is growing vertically, the asymptotic size effect is not $P/D^2 = \sigma_N \propto D^{-3/8}$ [105] but $\sigma_N \propto D^{-1/2}$. This was determined by a simplified analytical solution (with a uniform crack depth) by Dempsey *et al.* [54], and confirmed by a detailed numerical solution with a variable crack depth profile [23]. The latter also led to an approximate prediction formula for the entire practical range of D, which is of the type of Eq. 10 with $\sigma_N = 0$. This formula was shown to agree with the existing field test [59, 60, 81].

1.3.7.5 Reverse Size Effect in Buckling of Floating Ice or Cylindrical Shell

An interesting anomalous case is the size effect on the critical stress for elastic buckling of floating ice, i.e., a beam or plate on Winkler foundation. Consider floating ice pushing against an obstacle of size d in the horizontal direction. Dimensional analysis [102] suffices to determine the form of the buckling formula and the scaling. There are five variables in the problem, h = ice plate thickness, P_{cr}, E', ρ, h, d, and the solution must be have the form $F(P_{cr}, E', \rho, h, d,) = 0$, where P_{cr} = force applied on the obstacle, ρ = specific weight of sea water (or foundation modulus), and $E' = E/(1 - \nu^2)$, ν being the Poisson ratio. There are, however, only two independent physical dimensions in the problem, namely, the length and the force. Therefore, according to Buckingham's Π theorem of dimensional analysis [102], the solution must be expressible in terms of 5−2, i.e., 3 dimensionless parameters. They may be taken as $P_{cr}/E'hd$, $\sqrt{\rho D}/E'h$, and d/h, where $D = E'h^3/12$ = cylindrical stiffness of the ice plate. If the ice is treated as elastic, $P_{cr}/E'hd$ must be proportional to $\sqrt{\rho E'}/E'h$ and d/h. Denoting $\sigma_{Ncr} = P_{cr}/hd$ which represents the nominal buckling strength (or the average critical stress applied on the obstacle by the moving ice plate), we conclude that the buckling solution must have the form

$$\sigma_{Ncr} = \kappa(d/h)\sqrt{\rho E'}\sqrt{h} \tag{19}$$

where κ is a dimensionless parameter depending on d/h as well as the boundary conditions.

The interesting property of Eq. 19 is that σ_{Ncr} increases, rather than decreases, with ice thickness h. So there is a reverse size effect. Consequently, the buckling of the ice plate can control the force exerted on a stationary structure only when the plate is sufficiently thin. The reason for the reverse size effect is that the buckling wavelength (the distance between the inflexion points of the deflection profile), which is $L_{cr} = \pi(D/\rho)^{1/4}$ (as follows from dimensional analysis or nondimensionalization of the differential equation of plate buckling), is not proportional to h; rather, $L_{cr}/h \propto h^{-1/4}$, i.e., L_{cr} decreases with h. This contrasts with the structural buckling problems of columns, frames, and plates, in which L_{cr} is proportional to the structure size.

The axisymmetric buckling of a cylindrical shell under axial compression is a problem analogous to the beam on elastic foundation. Therefore, Eq. (refl-cr) must apply to it as well. Since the lowest critical stress for nonaxisymmetric buckling loads is nearly equal to that for the axisymmetric mode, the reverse size effect given by Eq. 19 must also apply.

1.3.7.6 Influence of Crack Separation Rate, Creep, and Viscosity

There are two mechanisms in which the loading rate affects fracture growth: (i) creep of the material outside the FPZ, and (ii) rate dependence of the severance of material bonds in the FPZ. The latter may be modeled as a rate process controlled by activation energy, with Arrhenius-type temperature dependence. This leads to a dependence of the softening stress-separation relation of the cohesive crack model on the rate of opening displacement. In an equivalent LEFM approach, the latter is modeled by considering the crack extension rate to be a power function of the ratio of the stress intensity factor to its critical R-curve value.

For quasi-brittle materials exhibiting creep (e.g., concretes and polymer composites, but not rocks or ceramics), the consequence of mechanism 1 (creep) is that a decrease of loading rate, or an increase of duration of a sustained load, causes a decrease of the effective length of the FPZ. This in turn means an increase of the brittleness number manifested by a leftward rigid-body shift of the size effect curve in the plot of log σ_N versus log D, i.e., a decrease of effective D_0. For slow or long-time loading, quasi-brittle structures become more brittle and exhibit a stronger size effect [26].

Mechanism 2 (rate dependence of separation) causes it to happen that an increase of loading rate, or a decrease of sustained load duration, leads to an upward vertical shift of the size effect curve for log σ_N but has no effect D_0 and thus on brittleness (this mechanism also explains an interesting recently discovered phenomenon — a reversal of softening to hardening after a sudden increase of the loading rate, which cannot be explained by creep).

So far all our discussions have dealt with statics. In dynamics problems, any type of viscosity η of the material (present in models for creep, viscoelasticity, or viscoplasticity) implies a characteristic length. Indeed, since η = stress/strainrate $\sim$ kg/m s, and the Young's modulus E and mass density ρ have dimensions $E \sim$ kg/m s^2 and $\rho \sim$ kg/m^3, the material length associated with viscosity is given by

$$\ell_v = \frac{\eta}{v\rho} \qquad v = \sqrt{\frac{E}{\rho}} \tag{20}$$

where v = wave velocity. Consequently, any rate dependence in the constitutive law implies a size effect (and a nonlocal behavior as well). There is, however, an important difference. Unlike the size effect associated with ℓ_0 or c_f, the viscosity-induced size effect (as well as the width of damage localization zones) is not time-independent. It varies with the rates of loading and deformation of the structure and vanishes as the rates drop to zero. For

this reason, an artificial viscosity or rate effect can approximate the nonviscous size effect and localization only within a narrow range of time delays and rates, but not generally.

1.3.7.7 Size Effect in Fatigue Crack Growth

Cracks slowly grow under fatigue (repeated) loading. This is for metals and ceramics described by the Paris (or Paris-Erdogan) law, which states that plot of the logarithm of the crack length increment per cycle versus the amplitude of the stress intensity factor is a rising straight line. For quasi-brittle material it turns out that a size increase causes this straight line to shift to the right, the shift being derivable from the size effect law in Eq. 10 ([BP] Sec. 11.7).

1.3.7.8 Size Effect for Cohesive Crack Model and Crack Band Model

The cohesive (or fictitious) crack model (called by Hillerborg *et al*. [68] and Petersson [93] the fictitious crack model) is more accurate yet less simple than the equivalent LEFM. It is based on the hypothesis that there exists a unique decreasing function $w = g(\sigma)$ relating the crack opening displacement w (separation of crack faces) to the crack bridging stress σ in the FPZ. The obvious way to determine the size effect is to solve $P_{\max}$ by numerical integration for step-by-step loading [93].

The size effect plot, however, can be solved directly if one inverts the problem, searching the size D for which a given relative crack length $\alpha = a/D$ corresponds to $P_{\max}$. This leads to the equations

$$D\int_{\alpha_0}^{\alpha} C^{\sigma\sigma}(\xi,\ \xi')v(\xi')\,d\xi' = -g'[\sigma(\xi)]v(\xi)$$
$$P_{\max} = \frac{\int_{\alpha_0}^{\alpha} v(\xi)d\xi}{D\int_{\alpha_0}^{\alpha} C^{\sigma P}(\xi)v(\xi)d\xi} \tag{21}$$

where the first represents an eigenvalue problem for a homogeneous Fredholm integral equation, with D as the eigenvalue and $v(\xi)$ as the eigenfunction; $\xi = x/D$, $x =$ coordinate along the crack (Fig. 1.3.6); $\alpha = a/D$, $\alpha_0 = a_0/D$; $a, a_0 =$ total crack length and traction-free crack length (or notch length); and $C^{\sigma\sigma}(\xi, \xi')$, $C^{\sigma P}(\xi) =$ compliance functions of structure for crack surface force and given load P. Choosing a sequence of α-values, for each one obtains from Eq. 21 the corresponding values of D and $P_{\max}$. These results have also been generalized to obtain directly the load and displacement corresponding, on

the load-deflection curve, to a point with any given tangential stiffness, including the displacement at the snapback point which characterizes the ductility of the structure.

The cohesive crack model possesses at least one, but for concrete typically two, independent characteristic lengths: $\ell_0 = EG_f/\sigma_0^2$ and $\ell_1 = EG_F/\sigma_0^2$ where G_F = area under the entire softening stress-displacement curve $\sigma = f(w)$, and G_f = area under the initial tangent to this curve, which is equal to G_F only if the curve is simplified as linear (typically $G_F \approx 2G_f$). The bilinear stress-displacement law used for concrete involves further parameters of the length dimension — the opening displacement w_f when the stress is reduced to zero at the displacement at the change of slope, but their values are implied by G_f, G_F, σ_0 and the stress at the change of slope.

The scatter of size effect measurements within a practicable size range (up to 1:30) normally does not permit identifying more than one characteristic length (measurements of postpeak behavior are used for that purpose). Vice versa, when only the maximum loads of structures in the bridging region between plasticity and LEFM are of interest, hardly more than one characteristic length (namely, c_f) is needed.

The crack band model, which is easier to implement is used in commercial codes (e.g., DIANA, SBETA) [49], is for localized cracking or fracture, nearly equivalent to the cohesive crack model ([BP], [97]), provided that the effective (average) transverse strain in the crack band is taken as $\varepsilon_y = w/h$ where h is the width of the band. All that has been said about the cohesive crack model also applies to the crack band model. Width h, of course,

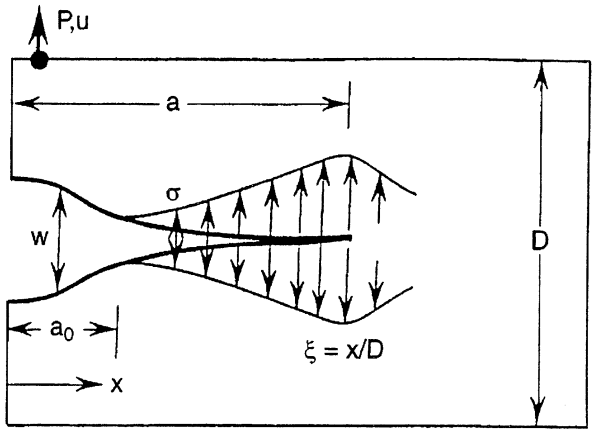

FIGURE 1.3.6 Cohesive crack and distribution of crack-bridging stresses.

represents an additional characteristic length, $\ell_4 = h$. It matters only when the cracking is not localized but distributed (e.g., due to the effect of dense and strong enough reinforcement), and it governs the spacings of parallel rocks. Their spacing cannot be unambiguously captured by the cohesive crack model.

1.3.7.9 Size Effect via Nonlocal, Gradient, or Discrete Element Models

The hypostatic feature of any model capable of bridging the power law size effects of plasticity and LEFM is the presence of some characteristic length, ℓ. In the equivalent LEFM associated with the size effect law in Eq. 10, c_f serves as a characteristic length of the material, although this length can equivalently be identified with δ_{CTOD} in Wells-Cottrell or Jenq-Shah models, or with the crack opening w_f at which the stress in the cohesive crack model (or crack band model) is reduced to zero (for size effect analysis with the cohesive crack model, see [BP] and Bažant and Li [25]).

In the integral-type nonlocal continuum damage models, ℓ represents the effective size of the representative volume of the material, which in turn plays the role of the effective size of the averaging domain in nonlocal material models. In the second-gradient nonlocal damage models, which may be derived as an approximation of the nonlocal damage models, a material length is involved in the relation of the strain to its Laplacian. In damage simulation by the discrete element (or random particle) models, the material length is represented by the statistical average of particle size.

The existence of ℓ in these models engenders a quasi-brittle size effect that bridges the power-law size effects of plasticity and LEFM and follows closely Eq. 10 with $\sigma_N = 0$, as documented by numerous finite element simulations. It also poses a lower bound on the energy dissipation during failure, prevents spurious excessive localization of softening continuum damage, and eliminates spurious mesh sensitivity ([BP], ch. 13).

These important subjects will not be discussed here any further because there exists a recent extensive review [ ].

1.3.7.10 Nonlocal Statistical Generalization of the Weibull Theory

Two cases need to be distinguished: (a) The front of the fracture that causes failure can be at only one place in the structure, or (b) the front can lie, with

different probabilities, at many different places. The former case occurs when a long crack whose path is dictated by fracture mechanics grows before the maximum load, or if a notch is cut in a test specimen. The latter case occurs when the maximum load is achieved at the initiation of fracture growth.

In both cases, the existence of a large FPZ calls for a modification of the Weibull concept: The failure probability P_1 at a given point of the continuous structure depends not on the local stress at that point, but on the nonlocal strain, which is calculated as the average of the local strains within the neighborhood of the point constituting the representative volume of the material. The nonlocal approach broadens the applicability of the Weibull concept to the case notches or long cracks, for which the existence of crack-tip singularity causes the classical Weibull probability integral to diverge at realistic m-values (in cleavage fracture of metals, the problem of crack singularity has been circumvented differently — by dividing the crack-tip plastic zone into small elements and superposing their Weibull contributions [77]).

Using the nonlocal Weibull theory, one can show that the proper statistical generalizations of Eq. 10 (with $\sigma_R = 0$) and Eq. 12 having the correct asymptotic forms for $D \to \infty$, $D \to 0$, and $m \to \infty$ are (Fig. 1.3.7):

$$\text{Case (a):} \quad \sigma_N = B\sigma_0(\beta^{2rn_d/m} + \beta^r)^{-1/2r} \qquad \beta = D/D_0 \tag{22}$$

$$\text{Case (b):} \quad \sigma_N = \sigma_0\zeta^{n_d/m}(1 + r\zeta^{1-rn_d/m})^{1/r} \qquad \zeta = D_b/D \tag{23}$$

where it is assumed that $rn_d < m$, which is normally the case.

The first formula, which was obtained for $r = 1$ by Bažant and Xi [36] and refined for $n \neq 1$ by Planas, has the property that the statistical influence on the size effect disappears asymptotically for large D. The reason is that, for long cracks or notches with stress singularity, a significant contribution to the Weibull probability integral comes only from the FPZ, whose size does not vary much with D. The second formula has the property that the statistical influence asymptotically disappears for small sizes. The reason is that the FPZ occupies much of the structure volume.

Numerical analyses of test data for concrete show that the size ranges in which the statistical influence on the size effect in case (a) as well as (b) would be significant do not lie within the range of practical interest. Thus the deterministic size effect dominates and its statistical correction in Eqs. 22 and 23 may be ignored for concrete, except in the rare situations where the deterministic size effect vanishes, which occurs rarely (e.g., for centric tension of an unreinforced bar).

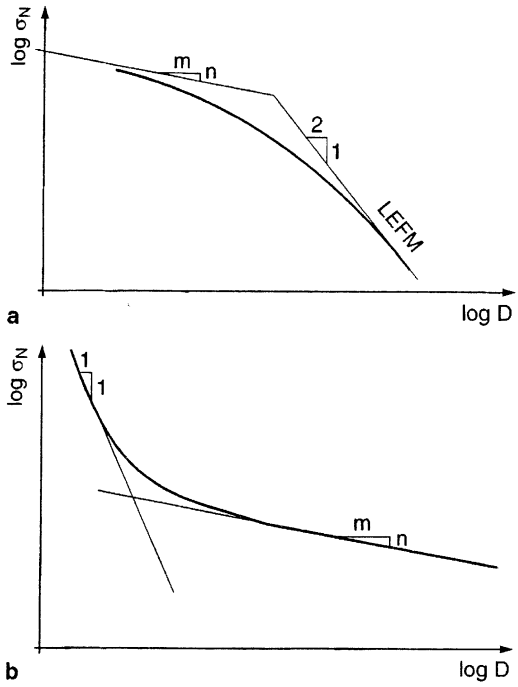

FIGURE 1.3.7 Scaling laws according to nonlocal generalization of Weibull theory for failures after long stable crack growth (top) or a crack initiation (right).

1.3.8 OTHER SIZE EFFECTS

1.3.8.1 Hypothesis of Fractal Origin of Size Effect

The partly fractal nature of crack surfaces and of the distribution of microcracks in concrete has recently been advanced as the physical origin of the size effects observed on concrete structures. Bhat [38] discussed a possible role of fractality in size effects in sea ice. Carpinteri [43, 44], Carpinteri and Ferro [38], Carpinteri *et al.* [45], and Carpinteri and Chiaia [46] proposed the so-called multifractal scaling law (MFSL) for failures occurring at fracture initiation from a smooth surface, which reads

$$\sigma_N = \sqrt{A_1 + (A_2/D)} \tag{24}$$

where A_1, A_2= constants. There are, however, four objections to the fractal theory [11]: (i) A mechanical analysis (of either invasive or lacunar fractals)

predicts a different size effect trend than Eq. 24, disagreeing with experimental observations. (ii) The fractality of the final fracture surface should not matter because typically about 99% of energy is dissipated by microcracks and frictional slips on the sides of this surface. (iii) The fractal theory does not predict how A_1 and A_2 should depend on the geometry of the structure, which makes the MFSL not too useful for design application. (iv) The MFSL is a special case of the second formula in Eq. 12 for $r = 2$, which logically follows from fracture mechanics;

$$A_1 = EG_f/c_f g'(0) \qquad A_2 = -EG_f g''(0)/2c_f[g'(0)]^3 \tag{25}$$

[12]. Unlike fractality, the fracture explanation of Eq. 24 has the advantage that, by virtue of these formulae, the geometry dependence of the size effect coefficients can be determined.

1.3.8.2 Boundary Layer, Singularity, and Diffusion

Aside from the statistical and quasi-brittle size effects, there are three further types of size effect that influence nominal strength:

1. The boundary layer effect, which is due to material heterogeneity (i.e., the fact that the surface layer of heterogeneous material such as concrete has a different composition because the aggregates cannot protrude through the surface), and to the Poisson effect (i.e., the fact that a plane strain state on planes parallel to the surface can exist in the core of the test specimen but not at its surface).
2. The existence of a three-dimensional stress singularity at the intersection of crack edge with a surface, which is also caused by the Poisson effect ([BP], Sec. 1.3). This causes the portion of the FPZ near the surface to behave differently from that in the interior.
3. The time-dependent size effects caused by diffusion phenomena such as the transport of heat or the transport of moisture and chemical agents in porous solids (this is manifested, e.g., in the effect of size on shrinkage and drying creep, due to size dependence of the drying half-time) and its effect on shrinkage cracking [96].

1.3.9 CLOSING REMARKS

Substantial though the recent progress has been, the understanding of the scaling problems of solid mechanics is nevertheless far from complete.

Mastering the size effect that bridges different behaviors on adjacent scales in the microstructure of material will be contingent upon the development of realistic material models that possess a material length (or characteristic length). The theory of nonlocal continuum damage will have to move beyond the present phenomenological approach based on isotropic spatial averaging, and take into account the directional and tensorial interactions between the effects causing nonlocality. A statistical description of such interactions will have to be developed. Discrete element models of the microstructure of fracturing or damaging materials will be needed to shed more light on the mechanics of what is actually happening inside the material and separate the important processes from the unimportant ones.

ACKNOWLEDGMENT

Preparation of the present review article was supported by the Office of Naval Research under Grant N00014-91-J-1109 to Northwestern University, monitored by Dr. Yapa D. S. Rajapakse.

REFERENCES AND BIBLIOGRAPHY

1. Argon, A. S. (1972). Fracture of composites, in *Treatise of Materials Science and Technology*, p. 79, vol. 1, New York: Academic Press.
2. Barenblatt, G. I. (1959). The formation of equilibrium cracks during brittle fracture. General ideas and hypothesis, axially symmetric cracks. *Prikl. Mat. Mekh.* **23** (3): 434–444.
3. Barenblatt, G. I. (1962). The mathematical theory of equilibrium cracks in brittle fracture. *Advanced Appl. Mech.* **7**: 55–129.
4. Bažant, Z. P. (1976). Instability, ductility, and size effect in strain-softening concrete. *J. Engrg. Mech. Div., Am. Soc. Civil Engrs.*, **102**: EM2, 331–344; disc. 103, 357–358, 775–777, 104, 501–502.
5. Bažant, Z. P. (1984). Size effect in blunt fracture: Concrete, rock, metal. *J. Engrg. Mech. ASCE* **110**: 518–535.
6. Bažant, Z. P. (1992). Large-scale thermal bending fracture of sea ice plates. *J. Geophysical Research*, **97** (C11): 17,739–17,751.
7. Bažant, Z. P. ed. (1992). *Fracture Mechanics of Concrete Structures*, Proc., First Intern. Conf. (FraMCoS-1), held in Breckenridge, Colorado, June 1–5, Elsevier, London (1040 pp.).
8. Bažant, Z. P. (1993). Scaling laws in mechanics of failure. *J. Engrg. Mech., ASCE* **119** (9): 1828–1844.
9. Bažant, Z. P. (1997a). Fracturing truss model: Size effect in shear failure of reinforced concrete. *J. Engrg. Mech., ASCE* **123** (12): 1276–1288.
10. Bažant, Z. P. (1997b). Scaling of quasibrittle fracture: Asymptotic analysis. *Int. J. Fracture* **83** (1): 19–40.
11. Bažant, Z. P. (1997c). Scaling of quasibrittle fracture: Hypotheses of invasive and lacunar fractality, their critique and Weibull connection. *Int. J. Fracture* **83** (1): 41–65.
12. Bažant, Z. P. (1998). Size effect in tensile and compression fracture of concrete structures: Computational modeling and design. *Fracture Mechanics of Concrete Structures* (3rd Int.

Conf., FraMCos-3, held in Gifu, Japan), H. Mihashi and K. Rokugo, eds., Aedificatio Publishers, Freiburg, Germany, 1905–1922.
13. Bažant, Z. P. (1999). Structural stability. *International Journal of Solids and Structures* **37** (200): 55–67; special issue of invited review articles on *Solid Mechanics* edited by G. J. Dvorak for U.S. Nat. Comm. on Theor. and Appl. Mech., publ. as a book by Elsevier Science, Ltd.
14. Bažant, Z. P. (1999). Size effect. *International Journal of Solids and Structures* **37** (200): 69–80; special issue of invited review articles on *Solid Mechanics* edited by G. J. Dvorak for U.S. Nat. Comm. on Theor. and Appl. Mech., Publ. as a book by Elsevier Science, Ltd.
15. Bažant, Z. P. (1999). Size effect on structural strength: A review. in *Archives of Applied Mechanics*, pp. 703–725, vol. 69, Berlin: Ingenieur-Orchiv, Springer Verlag.
16. Bažant, Z. P. (2000). Scaling laws for brittle failure of sea ice, *Preprints, IUTAM Symp. on Scaling Laws in Ice Mechanics* (Univ. of Alaska, Fairbanks, June), J. P. Dempsey, H. H. Shen, and L. H. Shapiro, eds., Paper No. 3, pp. 1–23.
17. Bažant, Z. P., and Cedolin, L. (1991). *Stability of Structures: Elastic, Inelastic, Fracture and Damage Theories* (textbook and reference volume), New York: Oxford University Press.
18. Bažant, Z. P., and Chen, E.-P. (1997). Scaling of structural failure. *Applied Mechanics Reviews, ASME* **50** (10): 593–627.
19. Bažant, Z. P., Daniel I. M., and Li, Zhengzhi (1996). Size effect and fracture characteristics of composite laminates. *ASME J. of Engrg. Materials and Technology* **118** (3): 317–324.
20. Bažant, Z. P., and Kazemi, M. T. (1990). Size effect in fracture of ceramics and its use to determine fracture energy and effective process zone length. *J. American Ceramic Society* **73** (7): 1841–1853.
21. Bažant, Z. P., and Kazemi, M. T. (1991). Size effect on diagonal shear failure of beams without stirrups. *ACI Structural Journal* **88** (3): 268–276.
22. Bažant, Z. P., Kim, J.-J. H., Daniel, I. M., Becq-Giraudon, E., and Zi, G. (1999). Size effect on compression strength of fiber composites failing by kink band propagation. *Int. J. of fracture* (special issue on Fracture Scaling, edited by Z. P. Bažant and Y. D. S. Rajapakse) (June), in press.
23. Bažant, Z. P., and Kim, J.-J. H. (1998). Size effect in penetration of sea ice plate with part-through cracks. I. Theory. *J. of Engrg. Mech., ASCE* **124** (12): 1310–1315; II. Results, *ibid.*, 1316–1324.
24. Bažant, Z. P., Kim, J.-J. H., Daniel, I. M., Becq-Giraudon, E., and Zi, G. (1999). Size effect on compression strength of fiber composites failing by kink band propagation. *Int. J. of Fracture*, in press.
25. Bažant, Z. P., and Li, Yuan-Neng (1997). Stability of cohesive crack model: Part I — Energy principles. *Tran. ASME, J. Applied Mechanics* **62**: 959–964; Part II — Eigenvalue analysis of size effect on strength and ductility of structures, *ibid.* **62**: 965–969.
26. Bažant, Z. P., and Li, Yuan-Neng (1997). Cohesive crack with rate-dependent opening and viscoelasticity: I. Mathematical model and scaling. *Int. J. Fracture* **86** (3): 247–265.
27. Bažant, Z. P., Lin, F.-B., and Lippmann, H. (1993). Fracture energy release and size effect in borehole breakout. *Int. Journal for Numerical and Analytical Methods in Geomechanics* **17**: 1–14.
28. Bažant, Z. P., and Novák, D. (2000). Probabilistic nonlocal theory for quasibrittle fracture initiation and size effect. I. Theory, and II. Application. *J. Engrg. Mech., ASCE* **126** (2): 166–174 and 175–185.
29. Bažant, Z. P., and Novák, D. (2000). Energetic-statistical size effect in quasibrittle materials. *ACI Materials Journal* **97** (3): 381–392.

30. Bažant, Z. P., and Oh, B.-H. (1983). Crack band theory for fracture of concrete. *Materials and Structures* (RILEM, Paris) **16**: 155–177.
31. Bažant, Z. P., and Pfeiffer, P. A. (1987). Determination of fracture energy from size effect and brittleness number. *ACI Materials J.* **84**: 463–480.
32. Bažant, Z. P., and Planas, J. (1998). *Fracture and Size Effect in Concrete and Other Quasibrittle Materials*, Boca Raton, Florida: CRC Press.
33. Bažant, Z. P., and Pfeiffer, P. A. (1987). Determination of fracture energy from size effect and brittleness number. *ACI Materials J.* **84**: 463–480.
34. Bažant, Z. P., and Vítek, J. L. (1999). Compound size effect in composite beams with softening connectors. I. Energy approach, and II. Differential equations and behavior. *J. Engrg. Mech., ASCE* **125** (11): 1308–1314 and 1315–1322.
35. Bažant, Z. P., and Rajapakse, Y. D. S., ed. (1999). *Fracture Scaling*, Dordrecht: Kluwer Academic Publishers (special issue of *Int. J. Fracture*), (June), in press.
36. Bažant, Z. P., and Xi, Y. (1991). Statistical size effect in quasi-brittle structures: II. Nonlocal theory. *ASCE J. Engineering Mechanics* **117** (11): 2623–2640.
37. Beremin, F. M. (1983). A local criterion for cleavage fracture of a nuclear pressure vessel steel. *Metallurgy Transactions A*, **14**: 2277–2287.
38. Bhat, S. U. (1990). Modeling of size effect in ice mechanics using fractal concepts. *Journal of Offshore Mechanics and Arctic Engineering* **112**: 370–376.
39. Budiansky, B. (1983). Micromechanics. *Computers and Structures* **16** (1–4): 3–12.
40. Budiansky, B., Fleck, N. A., and Amazigo, J. C. (1997). On kink-band propagation in fiber composites. *J. Mech. Phys. Solids* **46** (9): 1637–1635.
41. Carpinteri, A. (1986). *Mechanical damage and crack growth in concrete*, Dordrecht, Boston: Martinus Nijhoff — Kluwer.
42. Carpinteri, A. (1989). Decrease of apparent tensile and bending strength with specimen size: Two different explanations based on fracture mechanics. *Int. J. Solids Struct.* **25** (4): 407–429.
43. Carpinteri, A. (1994a). Fractal nature of material microstructure and size effects on apparent mechanical properties. *Mechanics of Materials* **18**: 89–101.
44. Carpinteri, A. (1994b). Scaling laws and renormalization groups for strength and toughness of disordered materials. *Int. J. Solids and Struct.* **31**: 291–302.
45. Carpinteri, A., Chiaia, B., and Ferro, G. (1994). Multifractal scaling law for the nominal strength variation of concrete structures. in *Size Effect in Concrete Structures* (Proc., Japan Concrete Institute International Workshop, held in Sendai, Japan, 1993), pp. 193–206, M. Mihashi, H. Okamura and Z.P. Bažant eds., London, New York: E & FN Spon.
46. Carpinteri, A., and Chiaia, B. (1995). in *Fracture Mechanics of Concrete Structures* (Proceedings of FraMCoS-2, held at ETH, Zürich), pp. 581–596, F. H. Wittmann, Freiburg: Aedificatió.
47. Carter, B. C. (1992). Size and stress gradient effects on fracture around cavities. *Rock Mech. and Rock Engng.* (Springer) **25** (3): 167–186.
48. Carter, B. C., Lajtai, E. Z., and Yuan, Y. (1992). Tensile fracture from circular cavities loaded in compression. *Int. J. Fracture* **57**: 221–236.
49. Červenka, V., and Pukl, R. (1994). SBETA analysis of size effect in concrete structures, in *Size Effect in Concrete Structures*, pp. 323–333, H. Mihashi, H. Okamura, and Z. P. Bažant, eds., London: E & FN Spon.
50. Cottrell, A. H. (1963). *Iron and Steel Institute Special Report* **69**: 281.
51. da Vinci, L. (1500s) — see *The Notebooks of Leonardo da Vinci* (1945), Edward McCurdy, London (p. 546); and *Les Manuscrits de Léonard de Vinci*, trans. in French by C. Ravaisson-Mollien, Institut de France (1881–91), vol. 3.

52. Dempsey, J. P., Adamson, R. M., and Mulmule, S. V. (1995a). Large-scale in-situ fracture of ice. vol. 1 (Proc., 2nd Int. Conf. on Fracture Mech. of Concrete Structures [FraMCoS-2], held at ETH, Zürich), pp. 575–684, F. H. Wittmann, ed., Freiburg: Aedificatió.
53. Dempsey, J. P., Adamson, R. M., and Mulmule, S. V. (1999). Scale effect on the in-situ tensile strength and failure of first-year sea ice at Resolute, NWR. *Int. J. Fracture* (special issue on Fracture Scaling), Z. P. Bažant and Y. D. S. Rajapakse, eds., in press.
54. Dempsey, J. P., Slepyan, L. I., and Shekhtman, I. I. (1995b). Radial cracking with closure. *Int. J. Fracture* **73** (3): 233–261.
55. Dugdale, D. S. (1960). Yielding of steel sheets containing slits. *J. Mech. Phys. Solids* **8**: 100–108.
56. Evans, A. G. (1978). A general approach for the statistical analysis of multiaxial fracture. *J. Am. Ceramic Soc.* **61**: 302–308.
57. Fréchet, M. (1927). Sur la loi de probabilité de l'écart maximum. *Ann. Soc. Polon. Math.* **6**: 93.
58. Fisher, R. A., and Tippett, L. H. C. (1928). Limiting forms of the frequency distribution of the largest and smallest member of a sample. *Proc., Cambridge Philosophical Society* **24**: 180–190.
59. Frankenstein, E. G. (1963). Load test data for lake ice sheet. *Technical Report 89*, U.S. Army Cold Regions Research and Engineering Laboratory, Hanover, New Hampshire.
60. Frankenstein, E. G. (1966). Strength of ice sheets. *Proc., Conf. on Ice Pressures against Struct.; Tech. Memor. No. 92, NRCC No. 9851*, Laval University, Quebec, National Research Council of Canada, Canada, pp. 79–87.
61. Freudenthal, A. M. (1956). Physical and statistical aspects of fatigue, in *Advance in Applied Mechanics*, pp. 117–157, vol. 4, New York: Academic Press.
62. Freudenthal, A. M. (1956). Statistical approach to brittle fracture, Chapter 6 in *Fracture*, vol. 2, pp. 591–619, H. Liebowitz, ed., New York: Academic Press.
63. Freudenthal, A. M., and Gumbell, E. J. (1956). Physical and statistical aspects of fatigue, in *Advances in Applied Mechanics*, pp. 117–157, vol. 4, New York: Academic Press.
64. Galileo, Galilei Linceo (1638). Discorsi i Demostrazioni Matematiche intorno à due Nuove Scienze, Elsevirii, Leiden; English trans. by T. Weston, London (1730), pp. 178–181.
65. Gettu, R., Bažant, Z. P., and Karr, M. E. (1990). Fracture properties and brittleness of high-strength concrete. *ACI Materials Journal* **87** (Nov.–Dec.): 608–618.
66. Griffith, A. A. (1921). The phenomena of rupture and flow in solids. *Phil. Trans.* **221A**: 179–180.
67. Haimson, B. C., and Herrick, C. G. (1989). In-situ stress calculation from borehole breakout experimental studies. *Proc., 26th U.S. Symp. on Rock Mech.*, 1207–1218.
68. Hillerborg, A., Modéer, M., and Petersson, P. E. (1976). Analysis of crack formation and crack growth in concrete by means of fracture mechanics and finite elements. *Cement and Concrete Research* **6**: 773–782.
69. Iguro, M., Shiyoa, T., Nojiri, Y., and Akiyama, H. (1985). Experimental studies on shear strength of large reinforced concrete beams under uniformly distributed load. *Concrete Library International, Japan Soc. of Civil Engrs*. No. **5**: 137–154. (translation of 1984 article in Proc. JSCE).
70. Jenq, Y. S., and Shah, S. P. (1985). A two parameter fracture model for concrete. *J. Engrg. Mech. ASCE*, **111** (4): 1227–1241.
71. Kani, G. N. J. (1967). Basic facts concerning shear failure. *ACI Journal, Proceeding* **64** (3, March): 128–141.
72. Kaplan, M.F. (1961). Crack propagation and the fracture concrete, *ACI J.* **58**, No. 11.
73. Kerr, A. D. (1996). Bearing capacity of floating ice covers subjected to static, moving, and oscillatory loads. *Appl. Mech. Reviews, ASME* **49** (11): 463–476.

74. Kesler, C. E., Naus, D. J., and Lott, J. L. (1971). Fracture mechanics — Its applicability to concrete, *Proc. Int. Conf. on the Mechanical Behavior of Materials*, pp. 113–124, vol. 4, Kyoto, The Soc. of Mater. Sci.
75. Kittl, P., and Diaz, G. (1988). Weibull's fracture statistics, or probabilistic strength of materials: State of the art. *Res. Mechanical*. **24**: 99–207.
76. Kittl, P., and Diaz, G. (1990). Size effect on fracture strength in the probabilistic strength of materials. *Reliability Engrg. Sys. Saf*. **28**: 9–21.
77. Lei, Y., O'Dowd, N. P., Busso, E. P., and Webster, G. A. (1998). Weibull stress solutions for 2-D cracks in elastic and elastic-plastic materials. *Int. J. Fracture* **89**: 245–268.
78. Leicester, R. H. (1969). The size effect of notches. *Proc., 2nd Australasian Conf. on Mech. of Struct. Mater.*, Melbourne, pp. 4.1–4.20.
79. Li, Yuan-Neng, and Bažant, Z. P. (1997). Cohesive crack with rate-dependent opening and viscoelasticity: II. Numerical algorithm, behavior and size effect. *Int. J. Fracture* **86** (3): 267–288.
80. Li, Zhengzhi, and Bažant, Z. P. (1998). Acoustic emissions in fracturing sea ice plate simulated by particle system. *J. Engrg. Mech. ASCE* **124** (1): 69–79.
81. Lichtenberger, G. J., Jones, J. W., Stegall, R. D., and Zadow, D. W. (1974). Static ice loading tests Resolute Bay — Winter 1973/74. *APOA Project No. 64, Rep. No. 745B-74-14, (CREEL Bib. No. 34-3095)*, Rechardson, Texas: Sunoco Sci. and Technol.
82. Mariotte, E. (1686). *Traité du mouvement des eaux*, posthumously edited by M. de la Hire; Engl. trans. by J. T. Desvaguliers, London (1718), p. 249; also *Mariotte's collected works*, 2nd ed., The Hague (1740).
83. Marti, P. (1989). Size effect in double-punch tests on concrete cylinders. *ACI Materials Journal* **86** (6): 597–601.
84. Mihashi, H. (1983). Stochastic theory for fracture of concrete, in *Fracture Mechanics of Concrete*, pp. 301–339, F. H. Wittmann, ed., Amsterdam: Elsevier Science Publishers.
85. Mihashi, H, and Izumi, M. (1977). Stochastic theory for concrete fracture. *Cem. Concr. Res*. **7**: 411–422.
86. Mihashi, H., Okamura, H., and Bažant, Z. P., eds., (1994). *Size Effect in Concrete Structures* (Proc., Japan Concrete Institute Intern. Workshop held in Sendai, Japan, Oct. 31–Nov. 2, 1995), London, New York: E & FN Spon.
87. Mihashi, H., and Rokugo, K., eds. (1998). *Fracture Mechanics of Concrete Structures* (Proc., 3rd Int. Conf., FraMCoS-3, held in Gifu, Japan), Freiburg: Aedificatio.
88. Mihashi, H., and Zaitsev, J. W. (1981). Statistical nature of crack propagation, Section 4-2 in *Report to RILEM TC 50* — FMC, F. H. Wittmann, ed.
89. Mulmule, S. V., Dempsey, J. P., and Adamson, R. M. (1995). Large-scale in-situ ice fracture experiments. Part II: Modeling efforts. *Ice Mechanics* — 1995 (ASME Joint Appl. Mechanics and Materials Summer Conf., held at University of California, Los Angeles, June), AMD-MD '95, New York: Am. Soc. of Mech. Engrs.
90. Nesetova, V., and Lajtai, E. Z. (1973). Fracture from compressive stress concentration around elastic flaws. *Int. J. Rock Mech. Mining Sci.* **10**: 265–284.
91. Okamura, H., and Maekawa, K. (1994). Experimental study of size effect in concrete structures, in *Size Effect in Concrete Structures*, pp. 3–24, H. Mihashi, H. Okamura, and Z. P. Bažant, eds., London: E & FN Spon (Proc. of JCI Intern. Workshop held in Sendai, Japan, 1993).
92. Peirce, F. T. (1926). *J. Textile Inst*. **17**: 355.
93. Petersson, P.E. (1981). Crack growth and development of fracture zones in plain concrete and similar materials. *Report* TVBM-1006, Div. of Building Materials, Lund Inst. of Tech., Lund, Sweden.

94. Planas, J., and Elices, M. (1988). Conceptual and experimental problems in the determination of the fracture energy of concrete. *Proc. Int. Workshop on Fracture Toughness and Fracture Energy, Test Methods of Concrete and Rock*. Tohoku Univ., Sendai, Japan, pp. 203–212.

95. Planas, J., and Elices, M. (1989). In *Cracking and Damage*, pp. 462–476, J. Mazars and Z. P. Bažant, eds., London: Elsevier.

96. Planas, J., and Elices, M. (1993). Drying shrinkage effects on the modulus of rupture, in *Creep and Shrinkage of Concrete* (Proc., 5th Int. RILEM Symp., Barcelona), pp. 357–368, Z. P. Bažant and I. Carol, eds., London: E & FN Spon.

97. Planas, J., Elices, M., and Guinea, G. V. (1983). Cohesive cracks vs. nonlocal models: Closing the gap. *Int. J. Fracture* **63** (2): 173–187.

98. Reinhardt, H. W. (1981). Masstabseinfluss bei Schubversuchen im Licht der Bruchmechanik. *Beton and Stahlbetonbau* (Berlin), No. 1, pp. 19–21.

99. RILEM Recommendation (1990). Size effect method for determining fracture energy and process zone of concrete. *Materials and Structures* **23**: 461–465.

100. Rosen, B. W. (1965). Mechanics of composite strengthening, *Fiber Composite Materials*, Am. Soc. for Metals Seminar, Chapter 3, American Society for Metals, Metals Park, Ohio, pp. 37–75.

101. Ruggieri, C., and Dodds, R. H. (1996). Transferability model for brittle fracture including constraint and ductile tearing effects — in probabilistic approach, *Int. J. Fracture* **79**: 309–340.

102. Sedov, L. I. (1959). *Similarity and Dimensional Methods in Mechanics*, New York: Academic Press.

103. *Selected Papers by Alfred M. Freudenthal* (1981). Am. Soc. of Civil Engrs., New York.

104. Shioya, Y., and Akiyama, H. (1994). Application to design of size effect in reinforced concrete structures, in *Size Effect in Concrete Structures* (Proc. of Intern. Workshop in Sendai, 1993), pp. 409–416, H. Mihashi, H. Okamura, and Z. P. Bažant, eds., London: E & FN Spon.

105. Slepyan, L.I. (1990). Modeling of fracture of sheet ice. *Izvestia AN SSSR, Mekh. Twrd. Tela* **25** (2): 151–157.

106. Sodhi, D. S. (1995). Breakthrough loads of floating ice sheets. *J. Cold Regions Engrg., ASCE* **9** (1): 4–20.

107. Tippett, L. H. C. (1925). On the extreme individuals and the range of samples. *Biometrika* **17**: 364.

108. von Mises. R. (1936). La distribution de la plus grande de *n* valeurs. *Rev. Math. Union Interbalcanique* **1**: 1.

109. Walraven, J., and Lehwalter (1994). Size effects in short beams loaded in shear. *ACI Structural Journal* **91** (5): 585–593.

110. Walraven, J. (1995). Size effects: their nature and their recognition in building codes. *Studi e Ricerche* (Politecnico di Milano) **16**: 113–134.

111. Walsh, P. F. (1972). Fracture of plain concrete. *Indian Concrete Journal* **46**, No. 11.

112. Walsh, P. F. (1976). Crack initiation in plain concrete. *Magazine of Concrete Research* **28**: 37–41.

113. Weibull, W. (1939). The phenomenon of rupture in solids. Proc., Royal Swedish Institute of Engineering Research (Ingenioersvetenskaps Akad. Handl.) **153**, Stockholm, 1–55.

114. Weibull, W. (1949). A statistical representation of fatigue failures in solids. *Proc., Roy. Inst. of Techn.* No. **27**.

115. Weibull, W. (1951). A statistical distribution function of wide applicability. *J Appl. Mech., ASME*, **18**.

116. Weibull, W. (1956). Basic aspects of fatigue. in *Proc., Colloquium on Fatigue*, Stockholm: Springer-Verlag.
117. Wells, A. A. (1961). Unstable crack propagation in metals-cleavage and fast fracture. *Symp. on Crack Propagation.* Cranfield, **1**: 210–230.
118. Williams, E. (1957). Some observations of Leonardo, Galileo, Mariotte and others relative to size effect, *Annals of Science* **13**: 23–29.
119. Wisnom, M. R. (1992). The relationship between tensile and flexural strength of unidirectional composite. *J. Composite Materials* **26**: 1173–1180.
120. Wittmann, F. H., ed. (1995). *Fracture Mechanics of concrete Structures* (Proc., 2nd Int. Conf. on Fracture Mech. of Concrete and Concrete Structures [FraMCoS-2]), held at ETH, Zurich), pp. 515–534, Freiburg: Aedificatio.
121. Wittmann, F. H., and Zaitsev, Yu.V. (1981). Crack propagation and fracture of composite materials such as concrete, in *Proc., 5th. Int. Conf. on Fracture* (ICF5), Cannes.
122. Zaitsev, J. W., and Wittmann, F. H. (1974). A statistical approach to the study of the mechanical behavior of porous materials under multiaxial state of stress, in *Proc. of the 1973 Symp. on Mechanical Behavior on Materials*, Kyoto, Japan.
123. Zech, B., and Wittmann, F. H. (1977). A complex study on the reliability assessment of the containment of a PWR, Part II. Probabilistic approach to describe the behavior of materials. in *Trans. 4th Int. Conf. on Structural Mechanics in Reactor Technology*, pp. 1–14, vol. H, J1/11, T. A. Jaeger and B. A. Boley, eds., Brussels: European Communities.